Table 1. Primer and probe sequences

Primer or probe	Specificity	Sequence (5'—3')
Real-time PCR		
CD81nt476F	CD81 exon 5	CCAGCACACTGACTGCTTTGA
CD81nt516R	CD81 exon 5	GCCCGAGGGACACAAATTG
CD81-1MGB probe	CD81 exon 5	CACCTCAGTGCTCAAG
419F	XMRV *gag*	ATCAGTTAACCTACCCGAGTCGGAC
518R	XMRV *gag*	CGCGGTTTCGGCGTAA
446MGB probe	XMRV *gag*	TTTGGAGTGGCTTTGTTGG
6173envF	XMRV *env*	GGCATACTGGAAGCCATCATCATC
6173envR	XMRV *env*	CCTGACCCTTAGGAGTGTTTCC
6173envMGB probe	XMRV *env*	ATGGGACCTAATTTCC
Nested PCR		
343F	XMRV *gag*	ACGAGTTCGTATTCCCGG
1131AR	XMRV *gag*	AGCCGCCTCTTCTTCATTGT
419F	XMRV *gag*	ATCAGTTAACCTACCCGAGTCGGAC
700R	XMRV *gag*	GTAACCCAGCGCCTCTTC
6080F	XMRV *env*	ATGTTTGCCCCGGTCATAC
6849R	XMRV *env*	ATTACACAGGGCCTGATGG
6173envF	XMRV *env*	GGCATACTGGAAGCCATCATCATC
6682envR	XMRV *env*	GCAGAGGTATGGTTGGAGTAAGTAC
PCR		
IAP-Forward	mouse IAP	ATAATCTGCGCATGAGCCAAGG
IAP-Reverse	mouse IAP	AGGAAGAACACCACAGACCAGA

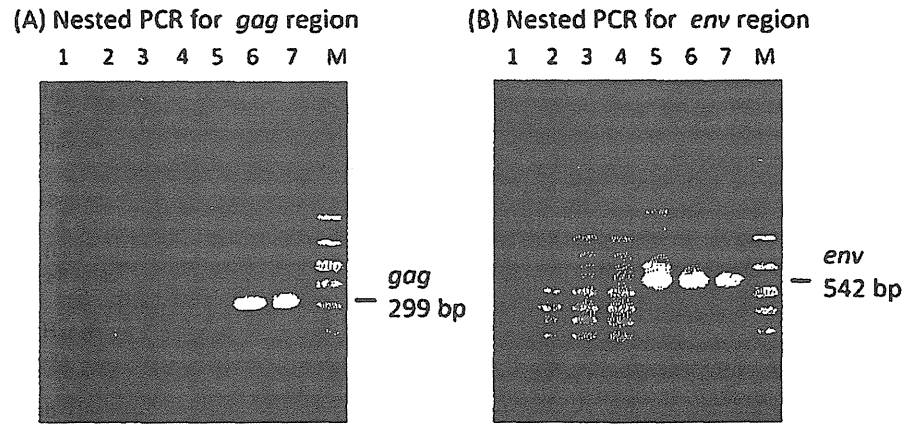

Fig. 1. Nested PCR for XMRV. DNA samples were amplified in the *gag* region (A) and *env* region (B). PCR products of H_2O as a negative control (lane 1), 1 μg of DNA from blood sample No. 75 (lanes 2, 3), 1 μg of real-time PCR-negative human DNA ([A] lanes 4, 5; [B] lane 4)), 50 and 5 copies of plasmid DNA harboring the *gag* region ([A] lanes 6, 7) and 500, 50, and 5 copies of plasmid DNA harboring the *env* region ([B] lanes 5, 6, 7). M indicates molecular marker.

respectively, which were spiked in 1 μg human DNA free of XMRV DNA, were detected by nested PCR. No amplification was apparent in either region in the 1 μg DNA of blood sample No. 75 (Fig. 1). The plasma fraction of blood sample No. 75 was subsequently subjected to Western blotting as described previously (8) to detect antibodies against XMRV; however, no antibodies were detected. These findings suggest that blood sample No. 75 did not contain XMRV DNA.

As XMRV and endogenous murine retroviral proviruses have very similar genomic sequences, mouse cellular DNA concealed in human nucleic acid samples can be amplified by PCR to detect XMRV. To confirm mouse DNA contamination in blood sample No. 75, we attempted to detect mouse intracisternal A-type particle (IAP) elements, which are high copy-number (approximately 1,000 copies per haploid genome), long-terminal repeat retrotransposons (9). DNA (1 μg) was subjected to PCR amplification using the IAP-forward and IAP-reverse primers (10). After 45 cycles of PCR amplification, the DNA obtained from the mouse fibroblast cell line L929, corresponding to 0.6 cells and 1 μg of human DNA, clearly produced amplified products. However, IAP did not get amplified in the DNA from blood sample No. 75. These results indicate that blood sample No. 75 was not contaminated by mouse cellular DNA. The weak amplification of XMRV in blood sample No. 75 by real-time PCR may be due to cross-reactions of the

primers and probes with similar sequences of human genomic DNA. Human chromosomes contain many retrovirus-like sequences (11), and some of these sequences are endogenous retroviruses. XMRV may have sequences similar to those in blood sample No. 75 with small mutations such as single nucleotide polymorphisms.

Some reports published over the past 2 years doubt that XMRV is a naturally occurring infection. Furthermore, contamination of the reagents used for PCR with mouse DNA, which contains MLV-like sequences has been reported (12). In additions, XMRV is present in some cell lines that are commonly handled in laboratories (13). Mouse genomic DNA contamination has also been found in human samples (10,14,15). These findings suggest that the initially observed high occurrence of XMRV infection is actually caused by contamination with mouse genomic DNA. Furthermore, XMRV may be the result of a recombination of two MLV ancestors in laboratories (16). In addition to the negative findings in CFS patients (17,18), it was demonstrated that there is no evidence of XMRV infection in blood donors in the USA (19). In Japan, Furuta et al. did not detect XMRV in CFS patients (8). In this study, we did not detect XMRV in donated blood in Japan. The findings of the present and previous studies did not confirm any association between XMRV and human diseases; this indicates that the risk of XMRV infection transmitted via transfusion is very low in Japan.

Acknowledgments We would like to thank Dr. Takashi Owada and Moe Kaneko for the culture of 22Rv1 cells.

Conflict of interest None to declare.

REFERENCES

1. Urisman, A., Molinaro, R.J., Fischer, N., et al. (2006): Identification of a novel gammaretrovirus in prostate tumors of patients homozygous for R462Q *RNASEL* variant. PLoS Pathog., 2, 211-225.
2. Lombardi, V.C., Ruscetti, F.W., Gupta, J.D., et al. (2009): Detection of an infection retrovirus, XMRV, in blood cells of patients with chronic fatigue syndrome. Science, 326, 585-588.
3. Switzer, W.M., Jia, H., Hohn, O., et al. (2010): Absence of evidence of xenotropic murine leukemia virus-related virus infection in persons with chronic fatigue syndrome and healthy controls in the United States. Retrovirology, 7, 57.
4. Kuppeveld F.J.M., Jong A.S., Lanke K.H., et al. (2010): Prevalence of xenotropic murine leukaemia virus-related virus in patients with chronic fatigue syndrome in the Netherlands: retrospective analysis of samples from an established cohort. Br. Med. J., 340, c1018.
5. Groom, H.C.T., Boucherit, V.C., Makinson K., et al. (2010): Absence of xenotopic murine leukaemia virus-related virus in UK patients with chronic fatigue syndrome. Retrovirology, 7, 10.
6. Rodriguez, J.J. and Goff, S.P. (2010): Xenotropic murine leukemia virus-related virus establishes an efficient spreading infection and exhibits enhanced transcriptional activity in prostate carcinoma cells. J. Viol., 84, 2556-2562.
7. Knouf, E.C., Metzger, M.J., Mitchell P.S., et al. (2009): Multiple integrated copies and high-level production of the human retrovirus XMRV (xenotropic murine leukemia virus-related virus) from 22Rv1 prostate carcinoma cells. J. Virol., 83, 7353-7356.
8. Furuta, R.A., Miyazawa, T., Sugiyama T., et al. (2011): No association of xenotropic murine leukemia virus-related virus with prostate cancer or chronic fatigue syndrome in Japan. Retrovirology, 8, 20.
9. Kuff, E.L. and Lueders, K.K. (1988): The intracisternal A-particle gene family: structure and functional aspects. Adv. Cancer Res., 51, 183-276.
10. Oakes, B., Tai, A.K., Cingöz, O., et al. (2010): Contamination of human DNA samples with mouse DNA can lead to false detection of XMRV-like sequences. Retrovirology, 7, 109.
11. Lander, E.S., Linton, L.M., Birren, B., et al. (2001): Initial sequencing and analysis of the human genome. Nature, 409, 860.
12. Sato, E., Furuta, R.A. and Miyazawa, T. (2010): An endogenous murine leukemia viral genome contaminant in a commercial RT-PCR kit is amplified using standard primers for XMRV. Retrovirology, 7, 110.
13. Takeuchi, Y., McClure, M.O. and Pizzato, M. (2008): Identification of gammaretroviruses constitutively released from cell lines used for human immunodeficiency virus research. J. Virol., 82, 12585-12588.
14. Robinson, M.J., Erlwein, O.W., Kaye, S., et al. (2010): Mouse DNA contamination in human tissue tested for XMRV. Retrovirology, 7, 108.
15. Hué, S., Gray, E.R., Gall, A., et al. (2010): Disease-associated XMRV sequences are consistent with laboratory contamination. Retrovirology, 7, 111.
16. Paprotka, T., Delviks-Frankenberry, K.A., Cingöz, O., et al. (2011): Recombinant origin of the retrovirus XMRV. Science, 333, 97-101.
17. Knox, K., Carrigan, D., Simmons, G., et al. (2011): No evidence of murine-like gammaretroviruses in CFS patients previously identified as XMRV-infected. Science, 333, 94-97.
18. Steffen, I., Tyrrell, D.L., Stein, E., et al. (2011): No evidence for XMRV nucleic acids, infections virus or anti-XMRV antibodies in Canadian patients with chronic fatigue syndrome. PLoS ONE. 6, e27870.
19. Dodd, R.Y., Hackett, J., Jr., Linnen, J.M., et al. (2012): Xenotropic murine leukemia virus-related virus does not pose a risk to blood recipient safety. Transfusion, 52, 298-306.

PLOS ONE

The CD3 versus CD7 Plot in Multicolor Flow Cytometry Reflects Progression of Disease Stage in Patients Infected with HTLV-I

Seiichiro Kobayashi[1], Yamin Tian[1,2], Nobuhiro Ohno[3], Koichiro Yuji[3], Tomohiro Ishigaki[4], Masamichi Isobe[3], Mayuko Tsuda[3], Naoki Oyaizu[5], Eri Watanabe[4], Nobukazu Watanabe[4], Kenzaburo Tani[2], Arinobu Tojo[1,3], Kaoru Uchimaru[3]*

1 Division of Molecular Therapy, Institute of Medical Science, The University of Tokyo, Tokyo, Japan, **2** Department of Molecular Genetics, Medical Institute of Bioregulation, Kyushu University, Fukuoka, Japan, **3** Department of Hematology/Oncology, Research Hospital, Institute of Medical Science, The University of Tokyo, Tokyo, Japan, **4** Laboratory of Diagnostic Medicine, Division of Stem Cell Therapy, Institute of Medical Science, The University of Tokyo, Tokyo, Japan, **5** Clinical Laboratory, Research Hospital, Institute of Medical Science, The University of Tokyo, Tokyo, Japan

Abstract

Purpose: In a recent study to purify adult T-cell leukemia-lymphoma (ATL) cells from acute-type patients by flow cytometry, three subpopulations were observed in a CD3 versus CD7 plot (H: $CD3^{high}CD7^{high}$; D: $CD3^{dim}CD7^{dim}$; L: $CD3^{dim}CD7^{low}$). The majority of leukemia cells were enriched in the L subpopulation and the same clone was included in the D and L subpopulations, suggesting clonal evolution. In this study, we analyzed patients with indolent-type ATL and human T-cell leukemia virus type I (HTLV-I) asymptomatic carriers (ACs) to see whether the CD3 versus CD7 profile reflected progression in the properties of HTLV-I-infected cells.

Experimental Design: Using peripheral blood mononuclear cells from patient samples, we performed multi-color flow cytometry. Cells that underwent fluorescence-activated cell sorting were subjected to molecular analyses, including inverse long PCR.

Results: In the D(%) versus L(%) plot, patient data could largely be categorized into three groups (Group 1: AC; Group 2: smoldering- and chronic-type ATL; and Group 3: acute-type ATL). Some exceptions, however, were noted (*e.g.*, ACs in Group 2). In the follow-up of some patients, clinical disease progression correlated well with the CD3 versus CD7 profile. In clonality analysis, we clearly detected a major clone in the D and L subpopulations in ATL cases and, intriguingly, in some ACs in Group 2.

Conclusion: We propose that the CD3 versus CD7 plot reflects progression of disease stage in patients infected with HTLV-I. The CD3 versus CD7 profile will be a new indicator, along with high proviral load, for HTLV-I ACs in forecasting disease progression.

Citation: Kobayashi S, Tian Y, Ohno N, Yuji K, Ishigaki T, et al. (2013) The CD3 versus CD7 Plot in Multicolor Flow Cytometry Reflects Progression of Disease Stage in Patients Infected with HTLV-I. PLoS ONE 8(1): e53728. doi:10.1371/journal.pone.0053728

Editor: Jean-Pierre Vartanian, Institut Pasteur, France

Received August 31, 2012; **Accepted** December 4, 2012; **Published** January 22, 2013

Funding: This study was supported by the Ministry of Education, Culture, Sports, Science and Technology, Japan. The funders had no role in study design, data collection and analysis, decision to publish, or preparation of the manuscript.

Competing Interests: The authors have declared that no competing interests exist.

* E-mail: uchimaru@ims.u-tokyo.ac.jp

Introduction

Human T-cell leukemia virus type I (HTLV-I) is the agent that causes HTLV-I-associated diseases, such as adult T-cell leukemia-lymphoma (ATL), HTLV-I-associated myelopathy/tropical spastic paraparesis (HAM/TSP), and HTLV-I uveitis (HU) [1–3]. Approximately 10–20 million people are infected with the HTLV-I virus worldwide [4]. The lifetime risk of developing ATL is estimated to be approximately 2.5–5% [5,6]. ATL includes a spectrum of diseases that are referred to as smoldering-, chronic-, lymphoma-, and acute-type [7,8]. The chronic and smoldering types of ATL are considered indolent and are usually managed with watchful waiting until the disease progresses to aggressive (lymphoma- or acute-type) ATL [9]. Because the prognosis of ATL is poor with current treatment strategies, factors to forecast progression to ATL from asymptomatic carriers (ACs) have been researched [10–13] in the hope that they will be useful for preventive therapy under development in the early malignant stage.

Various cellular dysfunctions induced by viral genes (*e.g.*, tax and HBZ), genetic and epigenetic alterations, and the host immune system are considered to cooperatively contribute to leukemogenesis in ATL [14–16]. However, the complex mechanism may hinder determination of a clear mechanism of the pathology and make discovery of risk factors difficult. In a prospective nationwide study in Japan, high proviral load (VL,

Table 1. Clinical profile of patients infected with HTLV-I and normal controls.

Clinical sutype	Number of cases	Male	Female	Age (range)	WBC(/μl) (range)	Lymphocytes(%) (range)	Abnormal lymphocytes(%) (range)
HTLV-1 AC	40	12	28	49.9 (28–70)	5525 (2680–10360)	35.9 (22.4–59.5)	0.9 (0.0–4.4)
Smoldering	7	4	3	55.3 (43–77)	5944 (3680–8710)	32.5 (13.4–47.5)	5.8 (0.7–16.5)
Chronic	7	4	3	52.7 (37–60)	9180 (4070–12790)	45.8 (35.0–61.5)	9.2 (3.4–12.7)
Acute	13	4	9	58.8 (42–74)	15328 (4450–41480)	16.3 (1.7–50.5)	40.3 (3.0–89.6)
Normal controls	10	6	4	47.4 (27–66)	ND	ND	ND

WBC: white blood cells (normal range, 3500–9100/μl).
AC: asymptomatic carrier.
ND: analysis were not performed.
Average of age, WBC, lymphocytes (%) and abnormal lymphocytes (%) are shown.
The proportion of abonormal lymphocytes in peripheral blood WBCs was evaluated by morphological exmanination.
doi:10.1371/journal.pone.0053728.t001

over 4.17 copies/100 peripheral blood mononuclear cells) was found to be a major risk factor for HTLV-I AC developing into ATL [13]. Although VL indicates the proportion of HTLV-I-infected cells, it does not indicate size or degree of malignant progression in each clone; *i.e.*, it does not directly indicate progression of disease stage in HTLV-I infection. Moreover, the majority of ACs with high VL remained intact during the study period, indicating that a more accurate indicator of progression is needed.

In our recent study to purify monoclonal ATL cells from acute-type patients by flow cytometry, three subpopulations were observed in a CD3 versus CD7 plot of $CD4^+$ cells (H: $CD3^{high}CD7^{high}$, D: $CD3^{dim}CD7^{dim}$, L: $CD3^{dim}CD7^{low}$), and the majority of ATL cells were enriched in the L subpopulation [17]. Clonality analyses revealed that the D and L subpopulations contained the same clone, suggesting clonal evolution of HTLV-I-infected cells to ATL cells. From these findings, we speculated that the CD3 versus CD7 profile may reflect disease progression in HTLV-I infection. In this study, the CD3 versus CD7 profile by flow cytometry, combined with molecular (clonality and proviral load) characterizations, were analyzed in patients with various clinical subtypes (HTLV-I AC, and indolent and aggressive ATL). We found that the CD3 versus CD7 profile reflected disease progression of HTLV-I-infected cells to ATL cells. We also discuss the significance of this analysis as a novel risk indicator for HTLV-I ACs in forecasting progression to ATL.

Materials and Methods

Cell lines and patient samples

TL-Om1, an HTLV-I-infected cell line, established Dr. Hinuma's laboratory [18], was provided by Dr. Toshiki Watanabe (The University of Tokyo, Tokyo, Japan) and was cultured in RPMI-1640 medium containing 10% fetal bovine serum. Peripheral blood samples were collected from inpatients and outpatients at our hospital from August 2009 to November 2011. All patients with ATL were categorized according to Shimoyama's criteria [7,8]. Patients with various complications, such as autoimmune disorder and systemic infections, were excluded. Lymphoma-type patients were excluded because ATL cells are not considered to exist in peripheral blood of this clinical subtype. In patients with ATL receiving chemotherapy, blood samples were collected before treatment or during the recovery phase between chemotherapy sessions. Samples collected from 10 healthy volunteers (mean age: 47.4 years; range: 27–66 years) were used as normal controls.

The present study was approved by the research ethics committee of the institute of medical science, the university of Tokyo. Subjects provided written informed consent.

Flow cytometry and cell sorting

Peripheral blood mononuclear cells (PBMCs) were isolated from heparin-treated whole blood by density gradient centrifugation, as described previously [17]. Cells were stained using a combination of phycoerythrin (PE)-CD7, APC-Cy7-CD3, Pacific Blue-CD4, and Pacific Orange-CD14. Pacific Orange-CD14 was purchased from Caltag-Invitrogen (Carlsbad, CA). All other antibodies were obtained from BD BioSciences (San Jose, CA). Propidium iodide (PI; Sigma, St. Louis, MO) was added to the samples to stain dead cells immediately prior to flow cytometry. A BD FACS Aria instrument (BD Immunocytometry Systems, San Jose, CA) was used for all multicolor flow cytometry and cell sorting. Data were analyzed using the FlowJo software (Treestar, San Carlos, CA).

Quantification of HTLV-I proviral load by real-time quantitative polymerase chain reaction (PCR)

The HTLV-I proviral load in FACS-sorted PBMCs was quantified by real-time quantitative polymerase chain reaction (PCR; TaqMan method) using the ABI Prism 7000 sequence detection system (Applied Biosystems, Foster City, CA) as described previously [13,17]. Briefly, 50 ng of genomic DNA was extracted from human PBMCs using a QIAamp DNA blood Micro kit (Qiagen, Hilden, Germany). Triplicate samples of the DNA were amplified. Each PCR mixture, containing an HTLV-I pX region-specific primer pair at 0.1 μM (forward primer 5′-CGGATACCCAGTCTACGTGTT-3′ and reverse primer 5′-

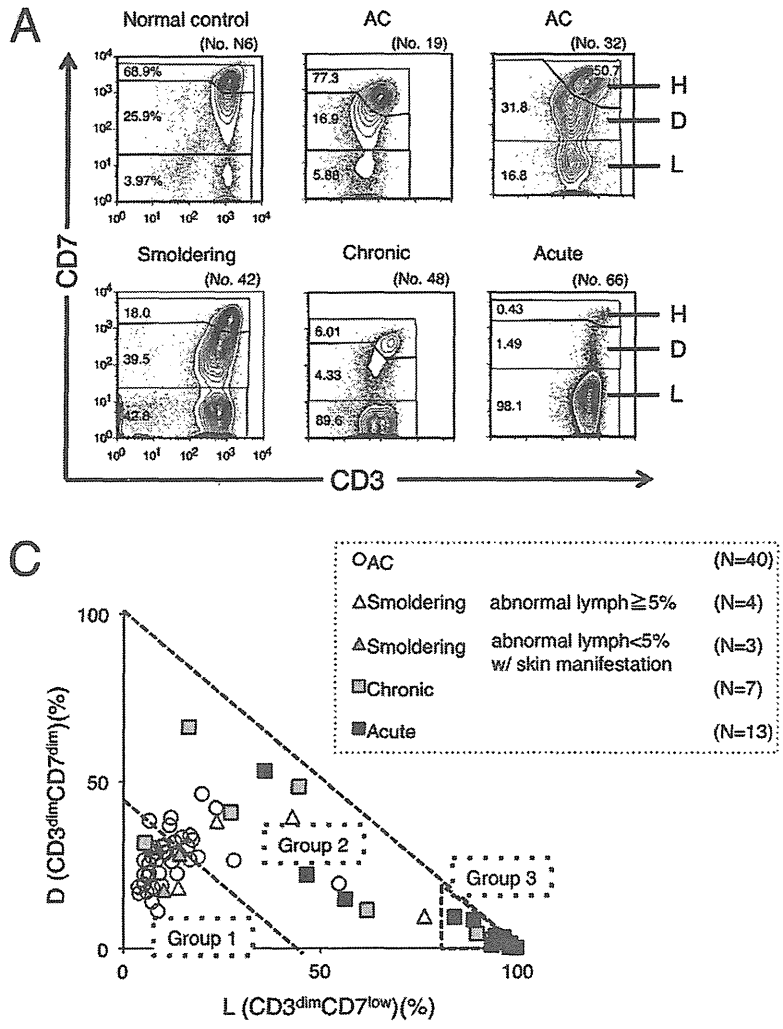

Figure 1. CD3 versus CD7 plots in flow cytometric analysis of patients who are asymptomatic HTLV-I carriers (ACs) and have various clinical subtypes of adult T-cell leukemia-lymphoma (ATL) suggest disease progression in HTLV-I infection. (A) Flow cytometric profile of an AC, various clinical subtypes of ATL (smoldering, chronic, and acute), and a normal control. Representative cases of CD3 versus CD7 plots in $CD4^+$ cells are shown. (B) A two-dimensional plot of AC cases showing the percentage of the D and L subpopulations by flow cytometry. AC cases were divided into two groups according to HTLV-I VL (greater or less than 4%). The border line (45% of D+L subpopulations) between Group 1 and 2 was set based on proviral load (VL). All AC cases with less than 4% VL were included in Group 1. All AC cases included in Group 2 had greater than 4% VL. VL<4%: n = 21; VL>4%: n = 19. All VL data in this figure were provided from the database of the Joint Study on Predisposing Factors of ATL Development (JSPFAD). (C) A two-dimensional plot of all patients showing the percentage of the D and L subpopulations. The smoldering type was divided into two categories: smoldering type with greater than 5% abnormal lymphocytes and smoldering type with less than 5% abnormal lymphocytes with skin manifestation. The two diagonal dotted lines indicate 45% and 100% of D+L subpopulations (*i.e.*, 55% and 0% of the H subpopulation). Data were categorized into three groups.
doi:10.1371/journal.pone.0053728.g001

CAGTAGGGCGTGACGATGTA-3′), FAM-labeled probe at 0.1 μM (5′- CTGTGTACAAGGCGACTGGTGCC-3′), and 1× TaqMan Universal PCR master mix (Applied Biosystems), was subjected to 50 cycles of denaturation (95°C, 15 seconds) and annealing to extension (60°C, 1 minute), following an initial Taq polymerase activation step (95°C, 10 minutes). The RNase P control reagent (Applied Biosystems) was used as an internal control for calculating the input cell number (using VIC reporter dye). DNAs extracted from TL-Om1 and normal human PBMCs were used as positive and negative controls, respectively. The HTLV-I proviral load (%) was calculated as the copy number of the pX region per input cell number. To correct the deviation of data acquired in each experiment, data from TL-Om1 (positive control) were adjusted to 100%, and the sample data were corrected accordingly by a proportional calculation.

Inverse long PCR

For clonality analysis, inverse long PCR was performed [17]. First, 1 μg of genomic DNA extracted from the FACS-sorted cells was digested with *Eco*RI and *Pst*I at 37°C overnight. Purification of DNA fragments was performed using a QIAEX2 gel extraction kit (Qiagen). The purified DNA was self-ligated with T4 DNA ligase (Takara Bio, Otsu, Japan) at 16°C overnight. The circular DNA obtained from the *Eco*RI digestion fragment was then digested

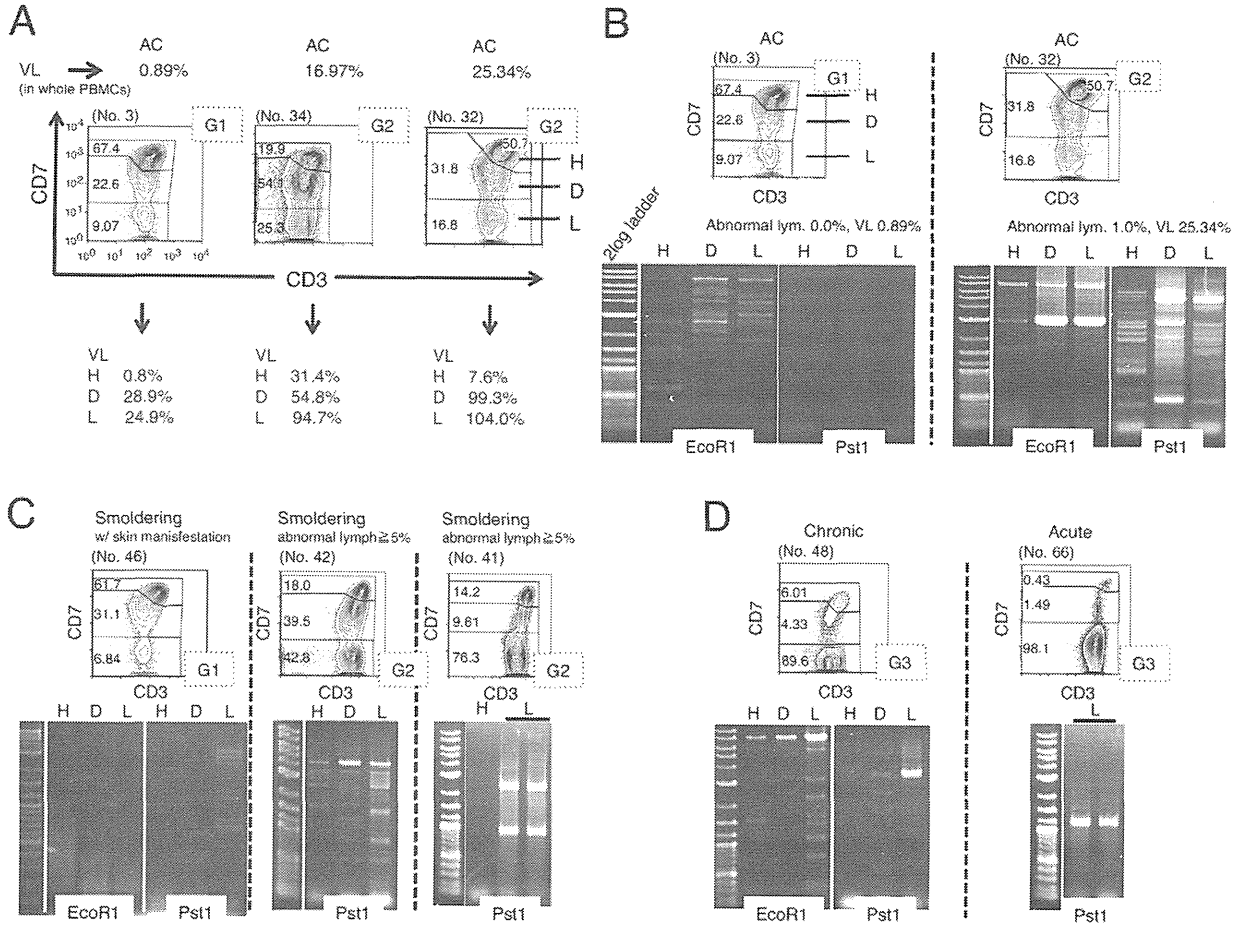

Figure 2. HTLV-I proviral load (VL) and clonality in each subpopulation, based on the CD3 versus CD7 plot. (A) The three subpopulations (H, D, L) based on the CD3 versus CD7 plot were subjected to fluorescence-activated cell sorting (FACS) and VL analysis. Three representative cases are shown. G1 or G2 in the dotted box indicates Group 1 or Group 2, categorized by the percentage of the D and L subpopulations, respectively. (B)–(D) Analysis of clonality in the three subpopulations based on the CD3 versus CD7 plot. Genomic DNA was extracted from FACS-sorted cells of each subpopulation and subjected to inverse long polymerase chain reaction (PCR). Representative data of two cases of AC (B), three cases of smoldering type, including one with skin manifestations (C), and cases of a chronic type and an acute type (D) are shown. PCR was performed in duplicate (black bars) in cases when a sufficient amount of DNA was obtained.
doi:10.1371/journal.pone.0053728.g002

with *Mlu*I, which cuts the pX region of the HTLV-I genome and prevents amplification of the viral genome. Inverse long PCR was performed using Takara LA *Taq* polymerase (Takara Bio). For the *Eco*RI-treated template, the forward primer was 5′-TGCCTGACCCTGCTTGCTCAACTCTACGTCTTTG-3′ and the reverse primer was 5′-AGTCTGGGCCCT-GACCTTTTCAGACTTCTGTTTC-3′. For the *Pst*I-treated group, the forward primer was 5′-CAGCCCATTCTATAG-CACTCTCCAGGAGAG-3′ and the reverse primer was 5′-CAGTCTCCAAACACGTAGACTGGGTATCCG-3. Each 50-μL reaction mixture contained 0.4 mM of each dNTP, 25 mM $MgCl_2$, 10× LA PCR buffer II containing 20 mM Tris-HCl and 100 mM KCl, 0.5 mM of each primer, 2.5 U LA *Taq* polymerase, and 50 ng of the processed genomic DNA. The reaction mixture was subjected to 35 cycles of denaturation (94°C, 30 seconds) and annealing to extension (68°C, 8 minutes). Following PCR, the products were subjected to electrophoresis on 0.8% agarose gels. In samples from which a sufficient amount of DNA was extracted, PCRs were performed in duplicate.

Results

CD3 versus CD7 profile in flow cytometry in various clinical subtypes of patients infected with HTLV-I

The clinical profiles of the 77 cases analyzed in this study are shown in Table 1. According to the gating procedure, as shown in Figure S1 [17], we constructed a CD3 versus CD7 plot of $CD4^+$ cells in PBMCs of various clinical subtypes from patients infected with HTLV-I and normal controls. The three subpopulations ($CD3^{high}CD7^{high}$, $CD3^{dim}CD7^{dim}$, and $CD3^{dim}CD7^{low}$) observed are referred to as the H, D, and L subpopulations, respectively. Representative results for each clinical subtype of HTLV-I infection are shown in Figure 1A. Regarding the data for an acute-type patient (no. 66), the dominant population was the L subpopulation, in which we previously demonstrated that monoclonal ATL cells are enriched [17]. Regarding the AC (no. 19), the CD3 versus CD7 profile was close to that of the normal control, although in some AC cases, such as no. 32, the profile differed from that of the normal control, because in contrast to case no. 19,

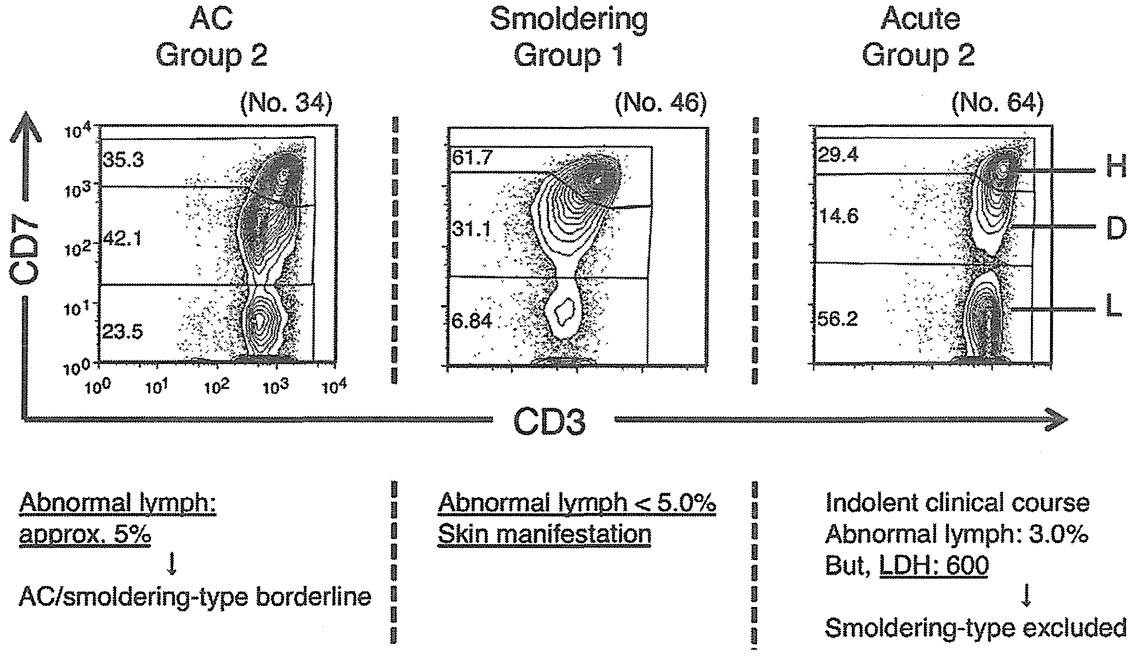

Figure 3. Study of exceptional cases categorized by proportion of the $CD3^{dim}CD7^{dim}$ (D) and $CD3^{dim}CD7^{low}$ (L) subpopulations. Left: An HTLV-I AC patient who was categorized in Group 2 in the D(%) versus L(%) plot. Middle: A patient with smoldering-type ATL who was categorized in Group 1. Right: A patient with acute-type ATL who was categorized in Group 2.
doi:10.1371/journal.pone.0053728.g003

these cases had increased D and L subpopulations. Regarding the data for indolent-type disease (smoldering and chronic), increases in the D and L subpopulations were intermediate between ACs and patients with acute-type disease. These representative flow cytometric data suggest that continuity in the CD3 versus CD7 profile seemed to exist among the various clinical subtypes of patients infected with HTLV-I.

The proportions of D and L subpopulations in all AC cases analyzed are shown in Figure 1B. Because the high HTLV-I proviral load (VL) in whole PBMCs, a VL of >4%, was reported to be a major risk indicator for progression to ATL [13], a border line was set based on VL. Group 1, the area under the diagonal line (D+L = 45%), included all AC cases with VLs of <4%. ACs with VLs of >4% were distributed between Groups 1 and 2. The proportions of D and L subpopulations in normal controls are shown in Figure S2. In this plot, all data for normal controls were distributed in Group 1. Data for all clinical subtypes are shown in Figure 1C. Most data for acute-type patients were located in the area beyond 80% of the L subpopulation and we designated this area as Group 3. Group 2, which is located between Group 1 and Group 3, included the majority of indolent-type (smoldering and chronic) cases. From these results, the three groups in the D(%) versus L(%) plot seemed to represent disease stage in each case.

Proviral load and clonality in each subpopulation in the CD3 versus CD7 plot

To further characterize each subpopulation (H, D, and L) in the CD3 versus CD7 plot, cells in each subpopulation were FACS-sorted and subjected to analysis of VL to determine the percentage of HTLV-I-infected cells in each subpopulation. Results for representative cases are shown in Figure 2A. The VL in whole PBMCs of an AC (no. 3) was low (0.89%). As expected, the VL in H, the major subpopulation, was low (0.8%). However, VLs in the D and L subpopulations were considerably higher (28.9% and 24.9%, respectively), indicating that HTLV-I-infected cells are relatively concentrated in these subpopulations. In the cases with high VLs in whole PBMCs (no. 32 with 25.34%; no. 34 with 16.97%), the VLs were also higher in the D and L subpopulations, and almost all cells in the L subpopulation were HTLV-I-infected.

In HTLV-I infection, progression to ATL requires several pathological steps, including clonal expansion [15]. To further characterize the three subpopulations based on the CD3 versus CD7 plot, we analyzed clonality in each subpopulation in patients with various clinical subtypes using the inverse long PCR method. Figure 2B shows two cases of AC. In the left case (no. 3), included in Group 1 in the D(%) and L(%) plot, multiple bands suggestive of multiple small clones were detected in the three subpopulations. However, no major band suggestive of a dominant clone was observed. In the right case (no. 32), included in Group 2, inverse long PCR of the FACS-sorted subpopulations suggested that the D and L subpopulations contained a major clone (Figure 2B). The D subpopulation had bands of the same size as those of the L subpopulation, indicating that the two distinct subpopulations contained a common major clone. Eleven cases of AC were included in Group 2. All three cases analyzed by Southern blotting (whole blood samples) were positive for clonal bands (Figure S3). In Figure 2C, data for three smoldering cases are shown. In case no. 46 (left), whose only manifestation was a skin eruption with few abnormal lymphocytes (less than 5% of white blood cells) in the peripheral blood, only faint minor bands suggestive of small clones were observed. In contrast, in the other two cases (nos. 42 and 41), intense bands suggestive of major clones were observed in both the D and L subpopulations. In no. 41 (right), weak bands were not visible, which suggested the selection of dominant clones. In Figure 2D, data for a chronic-type case and an acute-type case are shown. In both cases, intense bands in the L subpopulation suggest the existence of a major clone. The series of clonality analyses indicated that a major clone became more evident and the clinical

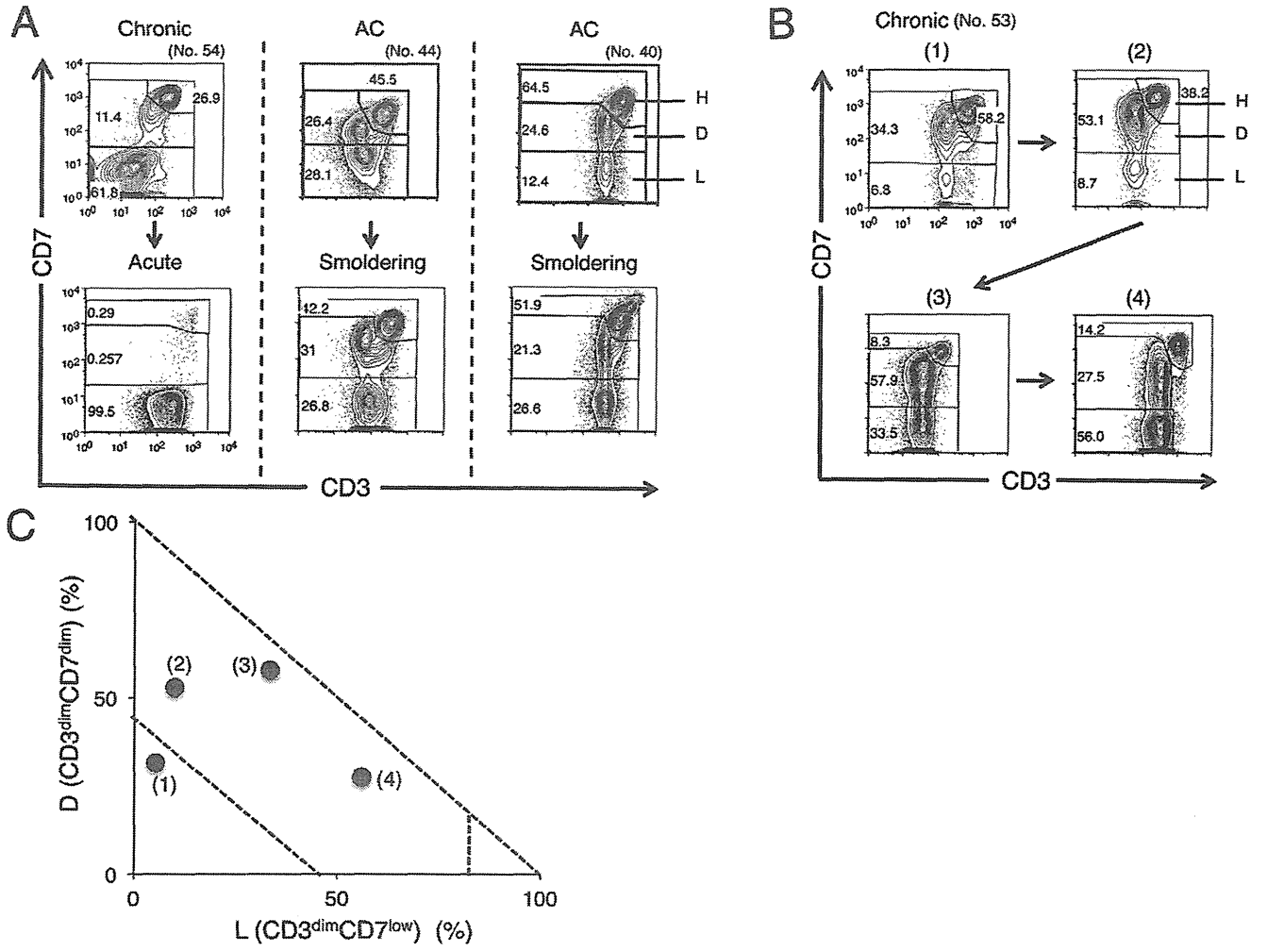

Figure 4. Alteration in the CD3 versus CD7 profile by flow cytometry in accordance with disease progression. (A) Change in the CD3 versus CD7 profile in representative cases. In all three cases shown, change in clinical data (*e.g.*, abnormal lymphocyte, LDH) resulted in progression of the clinical subtype. (B) Change in the CD3 versus CD7 profile in a time course in the case of chronic-type ATL. Clinical data are shown in Table S1. (C) Flow cytometric data in (B) are summarized in the D(%) versus L(%) plot.
doi:10.1371/journal.pone.0053728.g004

stage became more advanced as the D and L subpopulations increased.

Clinical evaluation of exceptional cases categorized by proportions of the $CD3^{dim}CD7^{dim}$ (D) and $CD3^{dim}CD7^{low}$ (L) subpopulations

As noted above, the D(%) versus L(%) plot generally represented disease stage in HTLV-I infection. However, we observed one case of chronic-type disease and three cases of smoldering-type disease in Group 1 and three cases of acute-type disease in Group 2. Furthermore, some ACs with VLs of >4% were observed in Group 2. Representative data from these apparently exceptional cases are shown in Figure 3. On the left, a case of AC (no. 34) observed in Group 2 is shown. 4.7% of lymphocytes in this blood sample were abnormal and clonality analysis by Southern blotting showed oligoclonal bands suggestive of clones of substantial size (Figure S3). These clinical data suggest that the disease stage would be around the AC/smoldering borderline. In the middle, a case of a smoldering type (no. 46) observed in Group 1 is shown. In this case, the percentage of abnormal lymphocytes in the peripheral blood was only 1%, but she had a histologically proven ATL lesion in the skin and was diagnosed with smoldering-type ATL. The other two smoldering cases categorized in Group 1 were the same as this case. These results indicate that ATL cells in these three smoldering cases infiltrated the skin, but not the peripheral blood. On the right, a case of acute-type disease categorized as Group 2 (no. 64) is shown. The clinical course of this patient was relatively indolent compared with typical acute-type disease. He had skin infiltration of ATL cells, but no lymph node swelling. However, LDH exceeded 1.5 times the upper limit of the normal range, which excludes a diagnosis of smoldering-type disease. Other acute-type cases categorized in Group 2 were diagnosed as such according to Shimoyama's criteria, but also had the same indolent clinical course as case no. 64. These cases should have been regarded as indolent ATL.

Changes in the CD3 versus CD7 profile in flow cytometry with disease progression

In several cases, we could obtain time-sequential samples (Figure 4). The patient (no. 54) shown on the left in Figure 4A progressed from chronic-type to acute-type disease. In flow cytometric analysis, decreases in the H and D subpopulations

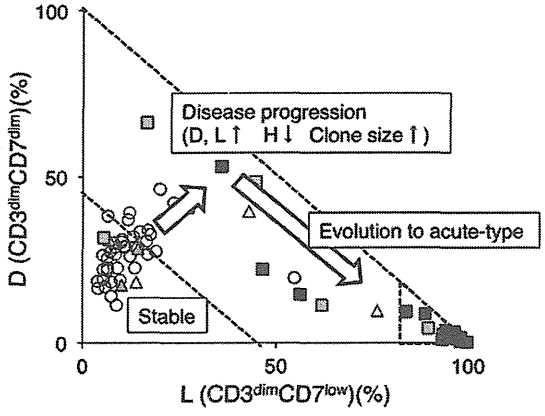

Figure 5. Summary of the study: the CD3 versus CD7 profile reflects progression of disease stage in patients infected with HTLV-I. In the percentage of D ($CD3^{dim}CD7^{dim}$) versus L ($CD3^{dim}CD7^{low}$) plot, Group 1 includes the majority of AC cases. As disease stage progresses, the CD3 versus CD7 profile then changes. With downregulation of CD3 and CD7, the D and L subpopulations increase gradually (Group 2). During this step, clones in the D and L subpopulations increase in size. Further accumulation of genetic alterations will result in rapid expansion of ATL clones—*i.e.*, evolution to acute-type ATL. In this step, the CD3 versus CD7 profile will progress from Group 2 to 3.
doi:10.1371/journal.pone.0053728.g005

and an increase in the L subpopulation were observed, indicating that disease progression correlated well with the change in the CD3 versus CD7 profile. The patients in the middle (no. 44) and on the right (no. 40) were included in Group 2 at the AC stage and later progressed to smoldering-type ATL. Although variation in the change of the flow cytometric profile was seen between these patients, the results suggest that ACs in Group 2 are at high risk of developing ATL.

The patient in Figure 4B (no. 53) was initially diagnosed with AC and later progressed to chronic-type ATL. Although the initial clinical course was stable, an increase in abnormal lymphocyte numbers was later observed, and low-dose VP-16 therapy (50 mg/day) was initiated because of hypoxemia due to lung infiltration of ATL cells. Table S1 and Figure 4C show summaries of the clinical data and the flow cytometric analyses, respectively. The flow cytometric data correlated well with disease progression.

Discussion

Findings in our previous analysis of acute-type ATL samples prompted our analysis of various clinical subtypes of patients infected with HTLV-I to examine whether the CD3 versus CD7 profile reflects the progression of oncogenesis in HTLV-I-infected cells [17]. Representative flow cytometric data shown in Figure 1A suggested that the CD3 versus CD7 profile changed during disease progression. As the disease stage progressed, the D and L subpopulations increased with concomitant decreases in the $CD3^{high}CD7^{high}$(H) subpopulation. Figure 1C, a summary of the flow cytometric data of all cases analyzed, reveals that the two-dimensional plot of the proportions of the D versus L subpopulations could divide all cases into three groups. Group 1, the area under the diagonal line, equivalent to 55% of the H subpopulation in which all normal controls were included (Figure S2), contained the majority of HTLV-I ACs. Group 3 was the area beyond 80% of the L subpopulation, and the majority of acute-type cases were included in this group. Group 2, located between Groups 1 and 3 (*i.e.*, less than 55% of the H subpopulation and 80% of the L subpopulation), included indolent-type (smoldering and chronic) cases and some AC cases. These results suggest that the CD3 versus CD7 expression profile reflects disease stage. Initially, both the D and L subpopulations gradually and simultaneously increased. However, at the clinically advanced stage, the increase in the L subpopulation was prominent. The change is considered to reflect the biological difference between the D and L subpopulations, which needs to be clarified.

In HTLV-I infection, the small clones of infected cells are considered to coexist from the AC stage [19,20]. A selected clone from the multiple small clones then grows and progresses to the malignant state, and the emergence of a dominant clone indicates disease progression in ATL [19,20]. As shown in Figure 2B–D, major bands suggesting dominant clones were evident in patients with progressed clinical subtypes or those in the advanced group in the CD3 versus CD7 profile, and major bands existed exclusively in the D and L subpopulations. These data also support the idea that increases in the D and L subpopulations correlate with the progression of disease stage. AC cases in Group 2 had high HTLV-I proviral loads (>4%; Figure 1B) and clear major bands were observed by inverse long PCR in these cases (Figure 2B, right). Sasaki *et al.* reported that two cases of HTVL-I AC with oligoclonal bands on Southern blots and high VLs (20%) had progressed to ATL by 4 and 3.5 years later [21]. The two cases may correspond to HTLV-I AC in Group 2 proposed in our study. In fact, two cases of ACs in our series that were included in Group 2 progressed to smoldering ATL (Figure 4A). AC cases in Group 2 could be regarded as advanced carriers. Our flow cytometric analysis could apparently discriminate high-risk AC cases from stable ones. Follow-up analysis of these cases is warranted to determine whether AC cases included in Group 2 progress to ATL. Flow cytometric data for these AC cases included in Group 2 (Figure 1A and 1C) were similar to those for indolent ATL cases in Group 2. These ACs in Group 2 can be considered essentially the same as smoldering ATL cases. Some of the ACs categorized according to Shimoyama's criteria should in fact be separated and regarded as a subtype together with at least some of the smoldering ATL cases.

Iwanaga *et al.* reported that high HTLV-I proviral load (>4%) in whole PBMCs was a risk factor for progression to ATL [13]. In Figure 1B, the ACs with VLs>4% were distributed between Groups 1 and 2. These findings suggest that not all ACs with high VLs are currently in an advanced stage, although they may have the potential to develop ATL in the future.

In general, the categorization by flow cytometric profile correlated well with the current classification of clinical subtypes, with some exceptional cases of acute-type and smoldering-type disease (Figure 3). The only manifestation of three smoldering cases categorized in Group 1 was skin lesions; they fell into Group 1 because they showed minimal abnormalities in peripheral blood [22]. Three acute-type ATL cases categorized in Group 2 had indolent clinical courses. A diagnosis of acute-type disease is made when the indolent-type and lymphoma-type are excluded, according to Shimoyama's criteria. The CD3 versus CD7 plot may discriminate the cases that will follow an indolent clinical course from the aggressive acute-type ATL.

The VL in each subpopulation indicated that HTLV-I-infected cells were relatively concentrated in the D and L subpopulations (representative data are shown in Figure 2A). These data are consistent with downregulation of CD3 and CD7 being relevant to HTLV-I infection, although cells without HTLV-I infection may also contribute to this change to some extent, as a substantial subpopulation of T cells has been reported to be CD7-deficient under physiological [23,24] and certain pathological conditions,

including autoimmune disorders and viral infection [25–29]. To more precisely analyze phenotypic changes in HTLV-I-infected cells, markers that indicate HTLV-I infection should be incorporated in future studies.

A summary of this study is shown in Figure 5. In the CD3 versus CD7 profile, most AC cases were included in Group 1, in which the D and L subpopulations were relatively small. Consistent with disease progression to smoldering- and chronic-type ATL, a decrease in the H subpopulation and increases in the D and L subpopulations occur (Group 2). In this step, increases in the sizes of clones in the D and L subpopulations are observed. Further expansion of the leukemic clone results in progression to acute-type ATL in which the L subpopulation has expanded (Group 3). According to a study by Yamaguchi *et al.*, the natural course of ATL is to progress from the HTLV-I carrier state through the intermediate state, smoldering ATL, and chronic ATL, and finally to the acute ATL, indicating a process of multistage leukemogenesis [19]. We consider this study to successfully link the progressive clinical status and phenotypic changes in HTLV-I-infected cells. However, the way in which this profile reflects multistep oncogenesis in HTVL-I infection at the molecular level remains unclear. Further molecular analyses of the three subpopulations will help in understanding the mechanism(s).

Supporting Information

Figure S1 Representative flow cytometric analysis of an HTLV-I asymptomatic carrier (patient no. 32). The CD3 versus CD7 plot of $CD4^+$ cells was constructed according to the gating procedure shown in this figure. In the plot, we designated three subpopulations: H ($CD3^{high}CD7^{high}$), D ($CD3^{dim}CD7^{dim}$), and L ($CD3^{dim}CD7^{low}$).
(PPTX)

Figure S2 A two-dimensional plot of 10 normal controls showing the percentage of the D and L subpopulations.
(PPTX)

Figure S3 Southern blot analysis of clonal integration of the HTLV-I provirus. Representative data (AC, No. 34) are shown. In *Eco*RI or *Pst*I digestion, a band indicated by a red arrow represents the monoclonal integration of the provirus. The band pattern indicates that two major clones coexist. This analysis was performed by a commercial laboratory (SRL, Tokyo, Japan).
(PPTX)

Table S1 Clinical data in a case of chronic-type ATL (No. 53). Proportion of abonormal lymphocytes in the peripheral blood WBC were evaluated by morphological exmanination. LDH: Lactate dehydrogenase (normal range, 120–240 U/L) sIL-2R: soluble interleukin-2 receptor (normal range, 122–496 U/ml).
(XLSX)

Acknowledgments

We thank Dr. Toshiki Watanabe, Dr. Kazumi Nakano, and Dr. Tadanori Yamochi (The University of Tokyo) for providing the TL-Om1 cell line and the plasmid containing the HTLV-I genome, which was used as a standard for the quantification of proviral load. We also thank Mr. Yuji Zaike (Clinical Laboratory, Research Hospital, Institute of Medical Science, The University of Tokyo) for his excellent technical advice. We are grateful to the hospital staff who have made a commitment to providing high-quality care to all of our patients.

Author Contributions

Conceived and designed the experiments: KT AT KU. Performed the experiments: SK YT. Analyzed the data: EW NW TI NO. Contributed reagents/materials/analysis tools: MI MT KU NO. Wrote the paper: SK KU.

References

1. Yoshida M, Miyoshi I, Hinuma Y (1982) Isolation and characterization of retrovirus from cell lines of human adult T-cell leukemia and its implication in the disease. Proc Natl Acad Sci U S A 79: 2031–2035.
2. Osame M, Usuku K, Izumo S, Ijichi N, Amitani H, et al. (1986) HTLV-I associated myelopathy, a new clinical entity. Lancet 1: 1031–1032.
3. Mochizuki M, Watanabe T, Yamaguchi K, Takatsuki K, Yoshimura K, et al. (1992) HTLV-I uveitis: a distinct clinical entity caused by HTLV-I. Japanese journal of cancer research : Gann 83: 236–239.
4. Proietti FA, Carneiro-Proietti AB, Catalan-Soares BC, Murphy EL (2005) Global epidemiology of HTLV-I infection and associated diseases. Oncogene 24: 6058–6068.
5. Yamaguchi K, Watanabe T (2002) Human T lymphotropic virus type-I and adult T-cell leukemia in Japan. International journal of hematology 76 Suppl 2: 240–245.
6. Murphy EL, Hanchard B, Figueroa JP, Gibbs WN, Lofters WS, et al. (1989) Modelling the risk of adult T-cell leukemia/lymphoma in persons infected with human T-lymphotropic virus type I. International journal of cancer Journal international du cancer 43: 250–253.
7. Shimoyama M (1991) Diagnostic criteria and classification of clinical subtypes of adult T-cell leukaemia-lymphoma. A report from the Lymphoma Study Group (1984–87). Br J Haematol 79: 428–437.
8. Tsukasaki K, Hermine O, Bazarbachi A, Ratner L, Ramos JC, et al. (2009) Definition, prognostic factors, treatment, and response criteria of adult T-cell leukemia-lymphoma: a proposal from an international consensus meeting. J Clin Oncol 27: 453–459.
9. Takasaki Y, Iwanaga M, Imaizumi Y, Tawara M, Joh T, et al. (2010) Long-term study of indolent adult T-cell leukemia-lymphoma. Blood 115: 4337–4343.
10. Hisada M, Okayama A, Shioiri S, Spiegelman DL, Stuver SO, et al. (1998) Risk factors for adult T-cell leukemia among carriers of human T-lymphotropic virus type I. Blood 92: 3557–3561.
11. Imaizumi Y, Iwanaga M, Tsukasaki K, Hata T, Tomonaga M, et al. (2005) Natural course of HTLV-1 carriers with monoclonal proliferation of T lymphocytes ("pre-ATL") in a 20-year follow-up study. Blood 105: 903–904.
12. Kamihira S, Atogami S, Sohda H, Momita S, Yamada Y, et al. (1994) Significance of soluble interleukin-2 receptor levels for evaluation of the progression of adult T-cell leukemia. Cancer 73: 2753–2758.
13. Iwanaga M, Watanabe T, Utsunomiya A, Okayama A, Uchimaru K, et al. (2010) Human T-cell leukemia virus type I (HTLV-1) proviral load and disease progression in asymptomatic HTLV-1 carriers: a nationwide prospective study in Japan. Blood 116: 1211–1219.
14. Okamoto T, Ohno Y, Tsugane S, Watanabe S, Shimoyama M, et al. (1989) Multi-step carcinogenesis model for adult T-cell leukemia. Japanese journal of cancer research : Gann 80: 191–195.
15. Matsuoka M, Jeang KT (2007) Human T-cell leukaemia virus type 1 (HTLV-1) infectivity and cellular transformation. Nat Rev Cancer 7: 270–280.
16. Yoshida M (2010) Molecular approach to human leukemia: isolation and characterization of the first human retrovirus HTLV-1 and its impact on tumorigenesis in adult T-cell leukemia. Proceedings of the Japan Academy Series B, Physical and biological sciences 86: 117–130.
17. Tian Y, Kobayashi S, Ohno N, Isobe M, Tsuda M, et al. (2011) Leukemic T cells are specifically enriched in a unique CD3(dim) CD7(low) subpopulation of CD4(+) T cells in acute-type adult T-cell leukemia. Cancer science 102: 569–577.
18. Sugamura K, Fujii M, Kannagi M, Sakitani M, Takeuchi M, et al. (1984) Cell surface phenotypes and expression of viral antigens of various human cell lines carrying human T-cell leukemia virus. International journal of cancer Journal international du cancer 34: 221–228.
19. Yamaguchi K, Kiyokawa T, Nakada K, Yul LS, Asou N, et al. (1988) Polyclonal integration of HTLV-I proviral DNA in lymphocytes from HTLV-I seropositive individuals: an intermediate state between the healthy carrier state and smouldering ATL. British journal of haematology 68: 169–174.
20. Mortreux F, Gabet AS, Wattel E (2003) Molecular and cellular aspects of HTLV-1 associated leukemogenesis in vivo. Leukemia : official journal of the Leukemia Society of America, Leukemia Research Fund, UK 17: 26–38.
21. Sasaki D, Doi Y, Hasegawa H, Yanagihara K, Tsukasaki K, et al. (2010) High human T cell leukemia virus type-1(HTLV-1) provirus load in patients with HTLV-1 carriers complicated with HTLV-1-unrelated disorders. Virology journal 7: 81.
22. Setoyama M, Katahira Y, Kanzaki T (1999) Clinicopathologic analysis of 124 cases of adult T-cell leukemia/lymphoma with cutaneous manifestations: the smouldering type with skin manifestations has a poorer prognosis than previously thought. The Journal of dermatology 26: 785–790.
23. Reinhold U, Abken H (1997) CD4+ CD7- T cells: a separate subpopulation of memory T cells? J Clin Immunol 17: 265–271.

24. Reinhold U, Abken H, Kukel S, Moll M, Muller R, et al. (1993) CD7- T cells represent a subset of normal human blood lymphocytes. J Immunol 150: 2081–2089.
25. Aandahl EM, Quigley MF, Moretto WJ, Moll M, Gonzalez VD, et al. (2004) Expansion of CD7(low) and CD7(negative) CD8 T-cell effector subsets in HIV-1 infection: correlation with antigenic load and reversion by antiretroviral treatment. Blood 104: 3672–3678.
26. Autran B, Legac E, Blanc C, Debre P (1995) A Th0/Th2-like function of CD4+CD7- T helper cells from normal donors and HIV-infected patients. J Immunol 154: 1408–1417.
27. Legac E, Autran B, Merle-Beral H, Katlama C, Debre P (1992) CD4+CD7-CD57+ T cells: a new T-lymphocyte subset expanded during human immunodeficiency virus infection. Blood 79: 1746–1753.
28. Schmidt D, Goronzy JJ, Weyand CM (1996) CD4+ CD7- CD28- T cells are expanded in rheumatoid arthritis and are characterized by autoreactivity. J Clin Invest 97: 2027–2037.
29. Willard-Gallo KE, Van de Keere F, Kettmann R (1990) A specific defect in CD3 gamma-chain gene transcription results in loss of T-cell receptor/CD3 expression late after human immunodeficiency virus infection of a CD4+ T-cell line. Proc Natl Acad Sci U S A 87: 6713–6717.

Satou et al. Retrovirology 2012, 9:46
http://www.retrovirology.com/content/9/1/46

RETROVIROLOGY

RESEARCH Open Access

HTLV-1 modulates the frequency and phenotype of FoxP3$^+$CD4$^+$ T cells in virus-infected individuals

Yorifumi Satou[1,5*], Atae Utsunomiya[2], Junko Tanabe[1], Masanori Nakagawa[3], Kisato Nosaka[4] and Masao Matsuoka[1*]

Abstract

Background: HTLV-1 utilizes CD4 T cells as the main host cell and maintains the proviral load via clonal proliferation of infected CD4$^+$ T cells. Infection of CD4$^+$ T cells by HTLV-1 is therefore thought to play a pivotal role in HTLV-1-related pathogenicity, including leukemia/lymphoma of CD4$^+$ T cells and chronic inflammatory diseases. Recently, it has been reported that a proportion of HTLV-1 infected CD4$^+$ T cells express FoxP3, a master molecule of regulatory T cells. However, crucial questions remain unanswered on the relationship between HTLV-1 infection and FoxP3 expression.

Results: To investigate the effect of HTLV-1 infection on CD4$^+$ T-cell subsets, we used flow cytometry to analyze the T-cell phenotype and HTLV-1 infection in peripheral mononuclear cells (PBMCs) of four groups of subjects, including 23 HTLV-1-infected asymptomatic carriers (AC), 10 patients with HTLV-1 associated myelopathy/tropical spastic paraparesis (HAM/TSP), 10 patients with adult T-cell leukemia (ATL), and 10 healthy donors. The frequency of FoxP3$^+$ cells in CD4$^+$ T cells in AC with high proviral load and patients with HAM/TSP or ATL was higher than that in uninfected individuals. The proviral load was positively correlated with the percentage of CD4$^+$ T cells that were FoxP3$^+$. The CD4$^+$FoxP3$^+$ T cells, themselves, were frequently infected with HTLV-1. We conclude that FoxP3$^+$ T-cells are disproportionately infected with HTLV-1 during chronic infection. We next focused on PBMCs of HAM/TSP patients. The expression levels of the T_{reg} associated molecules CTLA-4 and GITR were decreased in CD4$^+$FoxP3$^+$ T cells. Further we characterized FoxP3$^+$CD4$^+$ T-cell subsets by staining CD45RA and FoxP3, which revealed an increase in CD45RA$^-$FoxP3^{low} non-suppressive T-cells. These findings can reconcile the inflammatory phenotype of HAM/TSP with the observed increase in frequency of FoxP3$^+$ cells. Finally, we analyzed ATL cells and observed not only a high frequency of FoxP3 expression but also wide variation in FoxP3 expression level among individual cases.

Conclusions: HTLV-1 infection induces an abnormal frequency and phenotype of FoxP3$^+$CD4$^+$ T cells.

Keywords: HTLV-1, ATL, HAM/TSP, FoxP3, Tax, HBZ

Background

Human T-cell leukemia virus type 1 (HTLV-1) is a delta type retrovirus, which causes leukemia of HTLV-1-infected CD4$^+$ T cells, known as adult T-cell leukemia (ATL) [1-4], in 2 to 5 % of infected individuals. HTLV-1 is also associated with chronic inflammatory diseases [5,6], including HTLV-1 associated myelopathy/tropical spastic paraparesis (HAM/TSP), uveitis, alveolitis [7], and dermatitis [8]. It has been estimated that 20 million people are infected with HTLV-1 in the world. HTLV-1 has a characteristic proliferative strategy; HTLV-1 increases its copy number not via vigorous production of cell-free viral particle but mainly via proliferation of infected host cells, which contain the integrated HTLV-1 provirus in the host genome [9,10]. Given the fact that HTLV-1 utilizes CD4$^+$ T cells as the major host cell population, the pathogenesis by this virus may be due to abnormalities of CD4$^+$ T cells in HTLV-1-infected individuals. However the precise characteristics of the putative CD4$^+$ T-cell abnormality still remain to be elucidated.

In addition to viral structural proteins, such as Gag, Pol, and Env, HTLV-1 encodes several regulatory and

* Correspondence: y.satou@imperial.ac.uk; mmatsuok@virus.kyoto-u.ac.jp
[1]Laboratory of Virus Control, Institute for Virus Research, Kyoto University, Kyoto, 606-8507, Japan
[5]Current address: Immunology Section, Division of Infectious Diseases, Department of Medicine, Imperial College, London, W2 1PG, UK
Full list of author information is available at the end of the article

accessory proteins, including Tax, Rex, p30, p12, and HTLV-1 bZIP factor (HBZ), which regulate viral gene expression or proliferation of infected host cells [4]. After the HTLV-1 provirus is integrated into the host genome, the virus expresses these regulatory and accessory proteins to induce host cell proliferation or viral latency, resulting in persistent infection *in vivo*. Tax is known to influence various host cell-signaling pathways, for example activation of NF-κB, and to contribute to proliferation and survival of infected cells [11,12]. Another viral gene, the HBZ, which is encoded in the minus strand of HTLV-1 [13] and expressed constitutively in the infected host cells [14,15], also contributes to proliferation of the infected cells [14,16], dysregulation of differentiation and function of $CD4^+$ T cells [17], and the pathogenesis of diseases such as T-cell lymphoma and chronic inflammatory diseases [17,18]. On the other hand, viral protein expression induces the host immune response to eliminate the virus, which includes both antibody and cytotoxic T lymphocytes (CTL) against the viral antigens [19-21]. It has been reported that the CTL response against this virus determines HTLV-1 proviral load; yet, the host immune system cannot eliminate the HTLV-1 completely, which allows HTLV-1 to establish persistent infection in almost all infected individuals.

Recent studies have clarified the presence of various $CD4^+$ T-cell subsets. $CD4^+$ T cells can be divided into two major categories, effector T cells and regulatory T cells. Effector T cells induce the activation of immune responses by secreting pro-inflammatory cytokines whereas regulatory T cells, which express the transcription factor FoxP3 [22-24], suppress the immune response by both cell-contact dependent and independent mechanisms [25]. As an example of cell contact dependent suppression, expression of the immune suppressive molecule CTLA-4 on the cell surface inhibits the activation of surrounding neighboring T cells [26]. In addition, a recent report demonstrated that human $FoxP3^+CD4^+$ T cells were composed of three phenotypically and functionally different subsets according to the degree of FoxP3 expression and CD45RA expression, namely $CD45RA^+FoxP3^{low}$ resting T_{reg} cells (rT_{reg} cells), $CD45RA^-FoxP3^{high}$ activated T_{reg} cells (aT_{reg} cells), or $CD45RA^-FoxP3^{low}$ non-suppressive T cells ($FoxP3^{low}$ non-Treg cells) [27]. Both rT_{reg} cells and aT_{reg} cells have suppressive function, but $FoxP3^{low}$ non-Treg cells are not suppressive.

Previous studies have reported that the HTLV-1 provirus is enriched in effector/memory T cells [28,29], and the phenotype of ATL cells shares certain characteristics with regulatory T cells based on the finding of FoxP3 expression [30,31]. However there are few studies that systematically and specifically investigate which recently described $CD4^+$ T-cell subset is infected by HTLV-1 in asymptomatic carriers (AC), HAM/TSP patients, and ATL patients. To elucidate this point, we analyzed peripheral mononuclear cells (PBMCs) from naturally HTLV-1-infected individuals, including AC, HAM/TSP, and ATL patients, by using multicolor flow cytometric analysis combined with the detection of the viral antigen Tax to identify the presence of HTLV-1 [32]. We found the specific $CD4^+FoxP3^+$ T-cell subset is frequently infected with HTLV-1, which may allow the virus to achieve persistent infection *in vivo*, and should also contribute to the pathogenesis of the virus-associated diseases.

Results

The frequency of $FoxP3^+$ cells is positively correlated with HTLV-1 proviral load

Previous studies reported that the HTLV-1 provirus was frequently detected in effector/memory $CD4^+$ T cells [28], but at that time the analysis did not distinguish between effector/memory $CD4^+$ T cell and regulatory T cells (T_{reg} cells). Also further subsets of $CD4^+$ T cells have been identified recently, such as the division of $FoxP3^+CD4^+$ T cells into three distinct subsets [27]. In order to uncover the impact of HTLV-1 infection on the $CD4^+$ T-cell subset, it is necessary to re-evaluate the $CD4^+$ subsets in HTLV-1-infected individuals. We analyzed 23 ACs, 10 HAM/TSP patients, 10 ATL patients, and 10 healthy donors in this study as shown in Table 1. Almost all ATL cells express CD4, and indeed the percentage of $CD4^+$ T-cells in ATL patients was significantly higher than that of uninfected healthy donors ($p = 0.0051$, Figure 1A). There were no significant differences in the percentage of $CD4^+$ T cells between HD, AC, and HAM/TSP individuals ($p = 0.2153$ and 0.4597, respectively, Figure 1A). To characterize the $CD4^+$ T-cell subset in more detail, we stained PBMCs with anti-CD4, anti-CD45RA, and anti-FoxP3 antibodies. In this analysis we divided $CD4^+$ T cells into three distinct subsets, which include two $FoxP3^-$ populations ($CD45RA^+$ naïve T cells and $CD45RA^-$ effector/memory T cells) and a $FoxP3^+$ population. As shown in Figure 1B, the percentage of naïve $CD4^+$ T cells was decreased in ATL patients ($p = 0.0097$), but did not differ significantly between HD, AC and HAM/TSP ($p = 0.8381$ and 0.2567, respectively). The percentages of effector/memory $CD4^+$ T cells were not significantly different among the four studied subject groups (Figure 1C). However, frequencies of $FoxP3^+$ cells in HTLV-1 infected individuals (AC^{high}, ATL, HAM/TSP) were remarkably higher than those of HD ($p = 0.0054$, 0.0002 and 0.0002, respectively, Figure 1D). The frequencies of $FoxP3^+$ cells in AC were significantly correlated with HTLV-1 proviral load (PVL) ($r = 0.60$, $p = 0.0051$, Figure 1E). Additionally, the absolute number

Table 1 Characteristics of participants

Characteristics	HD	AC	ATL	HAM/TSP
Participant number	10	23	10	10
Age, median years (IQR)	54 (49–62)	59 (50–70)	65 (61–76)	60 (54–62)
Male sex, no (%)	3 (30)	6 (26)	5 (50)	3 (30)
WBC (IQR)/μL	4,930 (1,437)	5,157 (1,100)	17,030 (12,975)	5,900 (1,500)
Lymphocyte (IQR)/μL	1,717 (503)	1,697 (601)	8,443 (10,764)	1,739 (560)
PVL median (IQR)	-	1.8 (0.5–5.0)	59.6 (18.3–67.1)	9.6 (5.6–12.0)

NOTE. *HD* healthy donor; *AC* asymptomatic HTLV-1 carrier; *ATL* adult T-cell leukemia; *HAM/TSP* HTLV-1 associated myelopathy/tropic spastic paraparesis; *IQR* interquartile range; *PVL* proviral load. ATL patients consist of 2 acute, 4 smoldering and 4 chronic types of ATL cases.

of each T-cell subset showed the same tendency as well as the frequency (Additional file 1: Figure S1). These results collectively suggested that HTLV-1 infection increased the frequency of FoxP3$^+$CD4$^+$ T cells.

Tax expression after *ex vivo* culture is well correlated with proviral load

It has been reported that Tax expression increases spontaneously during *ex vivo* cultivation [32], which is useful to detect HTLV-1 infected cells at single cell level. We, therefore, used the same method to detect HTLV-1 infected cells by flow cytometry (Figure 2A), in which we can detect both Tax and various markers of CD4$^+$ T-cell subsets at the same time. We first evaluated the detection system by using a series of samples collected at different time points after *ex vivo* cultivation. We found that a small number of Tax-expressing cells could be detected after *ex vivo* cultivation for 6 hours; significant expression could be observed after 12 hours cultivation; and Tax expression continued for 24 hours of cultivation

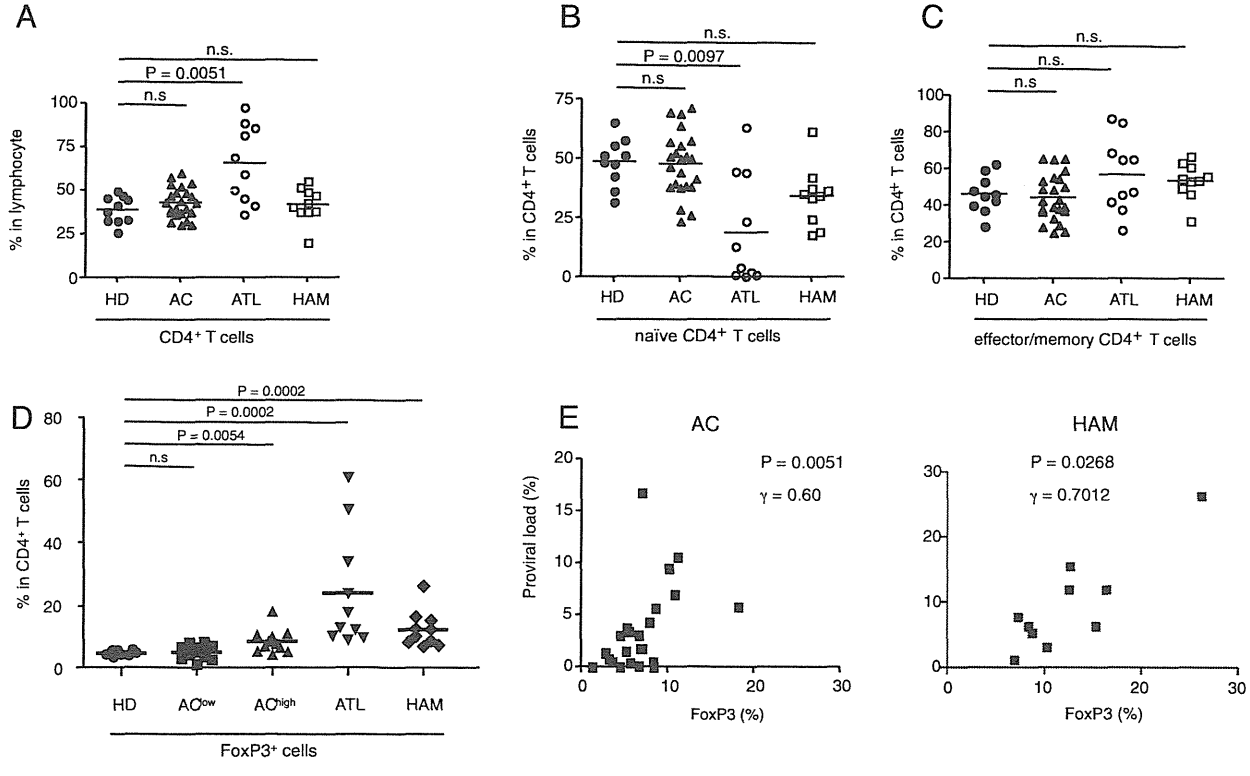

Figure 1 CD4$^+$T-cell subset in HTLV-1 infected individuals. (A) Percentages of CD4$^+$ T cells in 4 distinct subjects. Data shown are gated on lymphocyte fraction based on the dot plot pattern of SSC and FSC. **(B and C)** Proportion of FoxP3$^-$CD45RA$^+$ naïve CD4$^+$ T cells (B) or FoxP3$^-$CD45RA$^-$ effector/memory CD4$^+$ T cells (C). **(D)** Percentages of FoxP3$^+$ cells in CD4$^+$ T cells. **(E)** Frequency of FoxP3$^+$CD4$^+$ cells in ACs or HAM/TSP patients showed significant correlation with HTLV-1 proviral load by Spearman's rank correlation ($P = 0.0051$ or $P = 0.0268$, $r = 0.60$ or $r = 0.7012$, respectively).

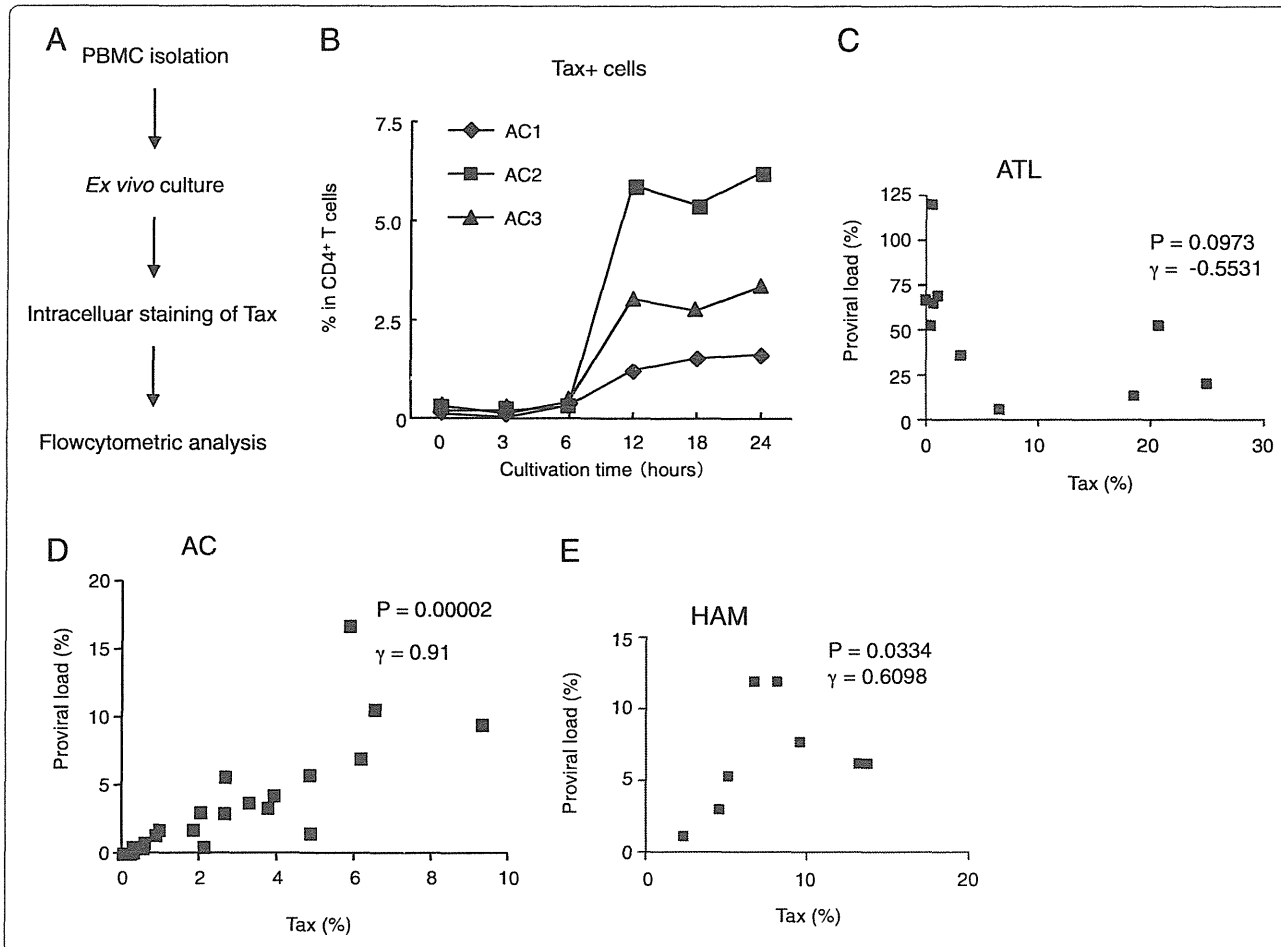

Figure 2 Characterization of Tax expression after *ex vivo* cultivation. (A) A flowchart of the experiment to detect Tax by flow cytometry. **(B)** The percentages of Tax expression in $CD4^+$ T cells after *ex vivo* culture are shown from 3 distinct ACs. **(C–E)** Correlation between Tax positivity in $CD4^+$ T cells and PVL in ATL patients (C), ACs (D) or HAM/TSP (E).

(Figure 2B). In order to confirm the efficiency of this system, we analyzed the correlation between HTLV-1 proviral load and the percentage of Tax expression in this system.

Consistent with previous reports that Tax expression is frequently silenced in ATL cells, Tax expression after *ex vivo* cultivation of ATL cells was not correlated with the proviral load (Figure 2C). The percentage of Tax positive cells tended to be lower than the proviral load even after *ex vivo* culture in AC and HAM/TSP patients, but we found that Tax positivity showed a significant correlation with the proviral load both in AC and HAM/TSP ($r = 0.91$ or 0.61, $p = 0.00002$ or 0.0334, respectively, Figure 2D and E). In order to investigate whether T-cell subset markers, including FoxP3 and CD45RA, are influenced by *ex vivo* cultivation, we analyzed their expression both before and after cultivation. The results showed that the frequency of FoxP3 or CD45RA was not significantly changed during *ex vivo* culture (Additional file2: Figure S2). These findings collectively indicate the usefulness of this Tax detection system for this study.

The frequency of HTLV-1 infection in each $CD4^+$ T-cell subset

We next investigated which T-cell subset is frequently infected with HTLV-1. We cultivated PBMCs isolated from HTLV-1 infected individuals *ex vivo* for 12–18 hours and stained with antibodies to Tax and various T-cell subset markers such as CD4, CD8, and FoxP3. Consistent with the previous reports, the frequency of Tax positivity in $CD4^+$ T cells was much higher than that in $CD8^+$ T cells ($p < 0.0001$, Figure 3A). Among $CD4^+$ T cells, the FoxP3 positive cell population contained a significantly higher ratio of Tax positive cells than that in FoxP3 negative cells ($p < 0.0001$, Figure 3B). In line with the finding in Figure 1E, the frequencies of $FoxP3^+$ cells were significantly correlated with Tax positivity in $CD4^+$ T cells. ($r = 0.48$, $p = 0.0257$, Figure 3C). These results indicated

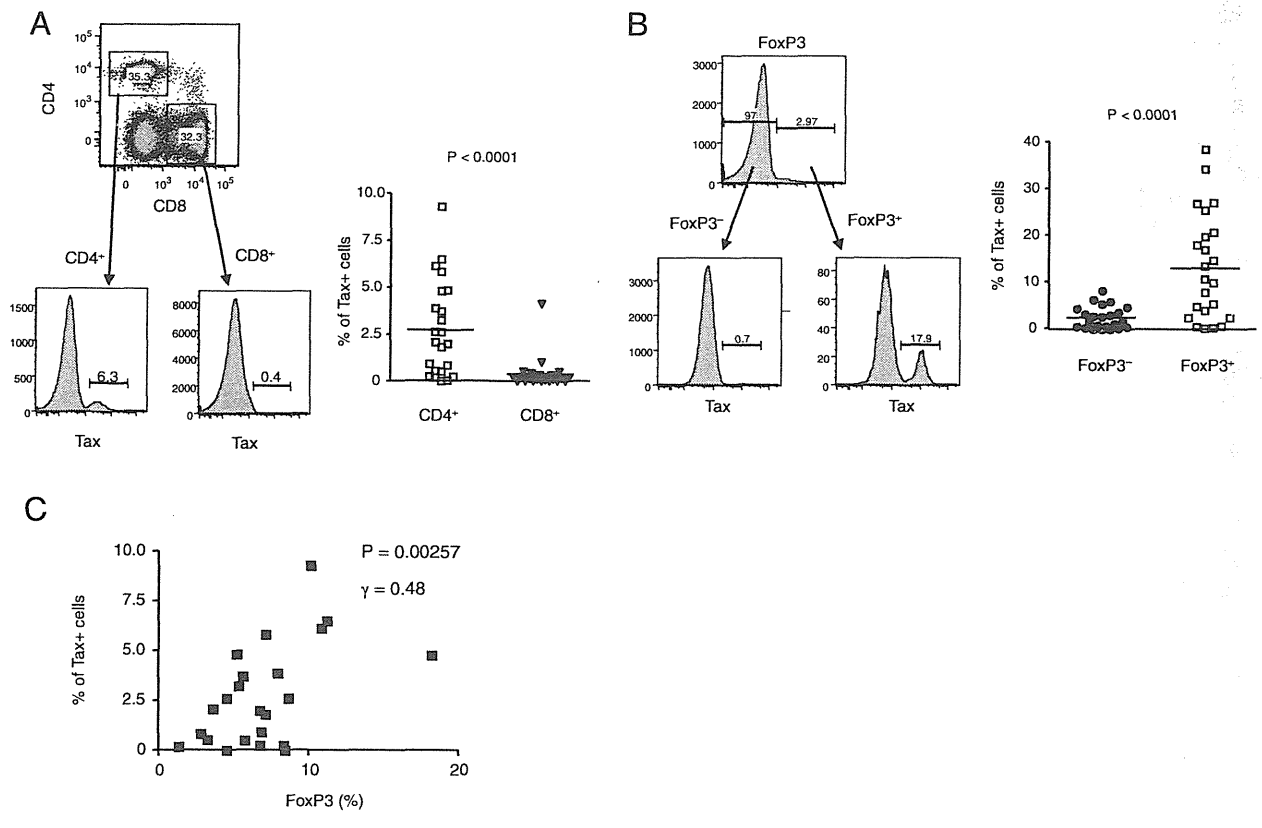

Figure 3 Frequency of HTLV-1-infection in each CD4$^+$ T-cell subset of asymptomatic HTLV-1 carriers. PBMCs from HTLV-1 asymptomatic carriers (n = 23) were cultivated for 18 hours, stained with anti-CD4, anti-CD8, anti-FoxP3, and anti-Tax antibodies, and analyzed by flow cytometry. **(A)** Representative dot plots of CD4 and CD8 and histograms of Tax in CD4$^+$ or CD8$^+$ T cells (Left panel). Right, cumulative results from 23 AC individuals are shown in graph (Right panel). **(B)** Representative histograms of Tax expression in FoxP3$^+$ or FoxP3$^-$ cell (Left panel). Right, cumulative results from 23 AC individuals are shown in graph (Right panel). **(C)** Tax positivity in CD4$^+$ T cells showed significant correlation with FoxP3 positivity in CD4$^+$ T cells by Spearman's rank correlation ($P = 0.0257$, r = 0.48).

that the increased FoxP3$^+$ cells in HTLV-1-infected individuals were frequently infected with HTLV-1.

Characterization of FoxP3$^+$CD4$^+$ T-cell subset in AC

We further focused on the FoxP3$^+$CD4$^+$ T-cell subset as defined previously (Figure 4A) [27]. First, we investigated the frequency of FoxP3$^+$CD4$^+$ T-cell subset in HD or AC. The results showed that the frequencies of rT_{reg} or aT_{reg} in AC^{low} or AC^{high} were not significantly different from that in HD (Figure 4B and 4 C), but $FoxP3^{low}$ non-T_{reg} cells were significantly more frequent in the AC^{high} population ($p = 0.0080$, Figure 4D). We next analyzed the presence of HTLV-1 in each CD4$^+$ T-cell subset by using AC sample. We observed that Tax positivity in FoxP3$^-$ effector/memory CD4$^+$ T cells was higher than that of FoxP3$^-$ naïve CD4$^+$ T cells ($p < 0.0001$, Figure 4E). Since effector/memory CD4 T cells are the most dominant in total CD4 T cells in terms of absolute cell number, the Tax-expressing cells are most abundant in effector/memory CD4 T cells (Additional file 3: Figure S3). More interestingly, Tax positivity in aT_{reg} cells or $FoxP3^{low}$ non-T_{reg} cells was much higher than that of rT_{reg} cells in ACboth AC^{low} and AC^{high} subjects ($p < 0.0001$ or 0.0001, respectively, Figure 4E). These results indicated that HTLV-1 is frequently present in aT_{reg} cells or $FoxP3^{low}$ non-T_{reg} cells.

Characteristics of T-cell subsets in HAM/TSP patients

To investigate the inflammatory aspects of HTLV-1 infection, we next focused on PBMCs of HAM/TSP patients. There were no significant differences in the percentage of CD4$^+$ or CD8$^+$ T cells between HD and HAM/TSP groups ($p = 0.3073$ and 0.1509, respectively, Figure 5A). The result of Tax staining showed that HTLV-1 infection was predominantly detected in CD4$^+$ T cells, and at a higher frequency in CD4$^+$FoxP3$^+$ T cells than CD4$^+$FoxP3$^-$ T cells ($p = 0.0069$, Figure 5B). To characterize the phenotype of FoxP3$^+$ cells in HAM/TSP patients, we investigated the expression levels of T_{reg} associated molecules, and found that the expression of GITR or CTLA-4 in HAM/TSP patients

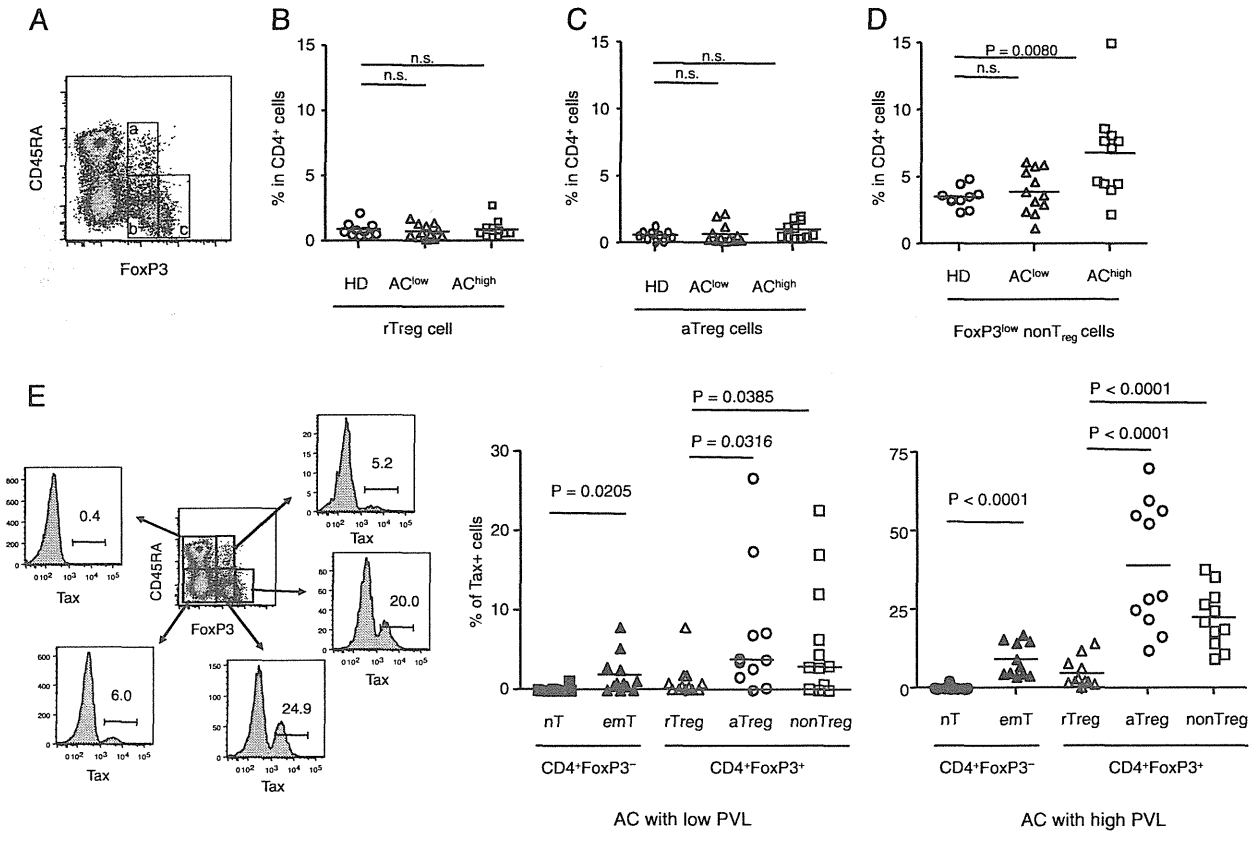

Figure 4 Characterization of FoxP3$^+$CD4$^+$ T-cell subset in AC samples. (A) A result of flow cytometric dot plots of CD45RA and FoxP3 in CD4$^+$ T cells of an AC sample is shown as an example. FoxP3$^+$CD4$^+$ T cells were classified into three subsets. a, CD45RA$^+$FoxP3^{low} resting T_{reg} cells (rT_{reg} cells); b, CD45RA$^-$FoxP3^{low} non-regulatory T cells (FoxP3^{low} non-T_{reg} cells), c, CD45RA$^-$FoxP3^{high} activated T_{reg} cells (aT_{reg} cells). **(B–D)** Frequencies of the FoxP3$^+$CD4$^+$ T-cell subset in HD, AC^{low}, and AC^{high}. Percentages of resting T_{reg} cells (B), activated T_{reg} cells (C), and FoxP3^{low} non-T_{reg} cells (D) in CD4$^+$ T cells are shown. **(E)** Representative flow cytometric dot plots of CD45RA and FoxP3 and histograms of Tax expression in each CD4$^+$ T-cell subset in an AC sample (Left panel). Cumulative results from 13 AC^{low} and 10 AC^{high} individuals are shown in the graph (Middle and right panels).

was significantly lower than that in HD ($p = 0.0328$ or 0.00002, respectively, Figure 5C). On the contrary, CD25 expression was high in HAM/TSP patients ($p = 0.0099$, Figure 5C). We further evaluated FoxP3$^+$CD4$^+$ T-cell subset in HAM/TSP patients. The frequencies of rT_{reg} were not significantly different from that in HD (p =0.9096, Figure 5D), but aT_{reg} cells or FoxP3^{low} non-T_{reg} cells were remarkably increased ($p = 0.0250$ or 0.0004, Figure 5E and 5F). Furthermore, aT_{reg} cells or FoxP3^{low} non-T_{reg} cells showed a high frequency of Tax + cells compared with rT_{reg} cells ($p = 0.0069$ or 0.0069, respectively, Figure 5G) as observed in ACs (Figure 4E). These data indicated that HTLV-1 infection significantly influenced not only the frequency but also the phenotype of CD4$^+$FoxP3$^+$ T cells in an inflammatory disease HAM/TSP.

Phenotypical analyses of ATL cells

Previous studies reported that some ATL cells express FoxP3 or CD25 [30,31,33], but the precise information about FoxP3$^+$CD4$^+$ T-cell subset of ATL cells remains unknown. We, therefore, analyzed CD4$^+$ T-cell subsets for ATL cases. FoxP3 positivity was 80% in ATL cases; yet the expression level was different among the cases (Figure 6A), which is consistent with previous reports [30,31]. In line with the finding in asymptomatic HTLV-1-infected carriers that the percentage of HTLV-1 in FoxP3^{low} non-T_{reg} cells or aT_{reg} cells was high (Figure 4E), ATL cells analyzed in this study did not express CD45RA, suggesting that FoxP3-expressing ATL cells might be derived from FoxP3^{low} non-T_{reg} or aT_{reg} cells. CD25 expression on ATL cells was generally high, but there was also much variation among the cases (Figure 6B).

Discussion

FoxP3$^+$ T_{reg} cells play a crucial role in persistent infection and pathogenesis of chronic viral infection. Previous studies have suggested that T_{reg} cells suppress virus-

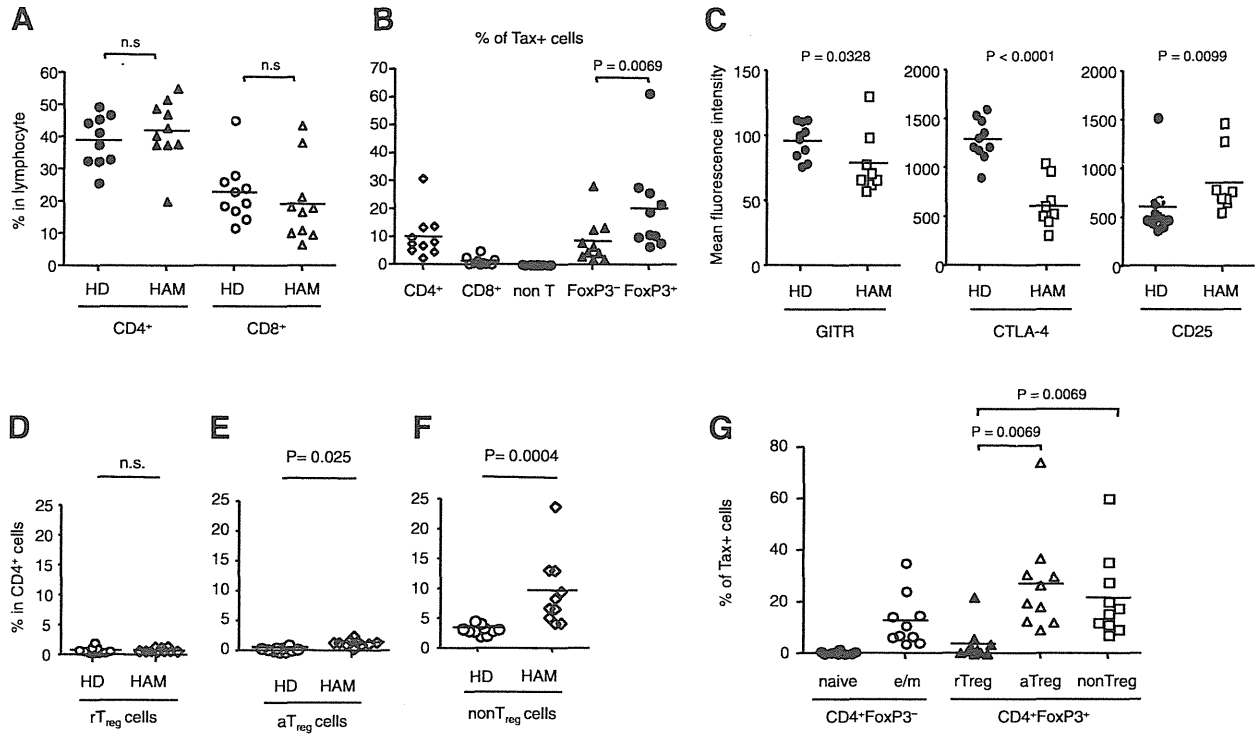

Figure 5 Detailed characterizations of CD4$^+$ T-cell subsets in HAM/TSP patients. Freshly isolated PBMCs from HAM/TSP patients (n = 10) were stained with anti-CD4, anti-CD45RA, anti-FoxP3 antibodies and analyzed by flow cytometry. To detect Tax expression, PBMCs were cultivated for 18 hours before antibody staining. **(A)** Percentages of CD4$^+$ or CD8$^+$ T cells in HAM/TSP patients. **(B)** Tax positivity of CD4$^+$, CD8$^+$, non-T, FoxP3$^-$, or FoxP3$^+$ cell populations in HAM/TSP patients. **(C)** Expression levels of T_{reg} associated molecules in FoxP3$^+$ cells of HD or HAM/TSP patients. **(D–F)** Frequencies of the FoxP3$^+$CD4$^+$ T-cell subset in HD and HAM/TSP patients. Percentages of rT_{reg} cells (D), aT_{reg} cells (E), and FoxP3^{low} non-T_{reg} cells (F) in CD4$^+$ T cells are shown. **(G)** Tax positivity of each CD4$^+$ T-cell subset in HAM/TSP patients.

specific CD8$^+$ T-cell effector functions in chronic human viral infections such as human immunodeficiency virus, hepatitis C virus and cytomegalovirus [34,35]. Regarding this point, FoxP3$^+$ T_{reg} cells play a role in facilitating viral persistence. In HTLV-1 infection, the frequency of FoxP3$^+$ cells is indeed correlated with the impairment of CTL activity against the viral antigen Tax in HAM/TSP patient [36]. On the other hand, FoxP3$^+$ T_{reg} cells could prevent tissue damage caused by excessive immune response triggered by viral infection. In addition to these general roles of FoxP3$^+$ T_{reg} cells in chronic viral infection, FoxP3$^+$ T_{reg} cells should have some specific role in HTLV-1 infection, because FoxP3$^+$ T_{reg} cells are comprised in CD4$^+$ T cells, which are a main host cell population of HTLV-1. Here we performed a comprehensive analysis of CD4$^+$ T-cell subsets in individuals naturally infected with HTLV-1 and revealed that the frequency of HTLV-1 infection is positively correlated with the frequency of FoxP3$^+$ T cells (Figure 1E). The increased FoxP3$^+$ T cells themselves are frequently infected with HTLV-1 (Figure 3B), suggesting that HTLV-1 utilizes the FoxP3$^+$ T cells as a host cell. What is the advantage for HTLV-1 to exist in FoxP3$^+$ T cells? There are two possibilities for this preference. First, FoxP3$^+$ T cells are known as hyper-proliferating cells *in vivo* with a doubling time of 8 days [37], which could contribute to clonal expansion of infected cells. Second, HTLV-1 can evade the host immune system by directly infecting this potentially immuno-suppressive cell population. Thus, HTLV-1-infection of FoxP3$^+$ T cells should enable the virus to increase or maintain proviral load and achieve persistent infection.

How then does HTLV-1 infection target FoxP3$^+$ T cells? This could be explained by the following two mechanisms. First, FoxP3$^+$ T cells are known to contact with dendritic cells (DCs) frequently [38], which could increase the chance of *de novo* viral infection between DCs and FoxP3$^+$ T cells. A recent study demonstrated that cell-free HTLV-1 efficiently infects DCs, and the infected DCs promote *de novo* infection of CD4$^+$ T cells [39]. This notion is consistent with the finding that effector/memory-type CD45RA$^-$ T_{reg} cells, including FoxP3^{low} non-T_{reg} cells and FoxP3^{high} aT_{reg} cells, are more frequently infected with HTLV-1 than CD45RA$^+$ rT_{reg} cells (Figure 4E). Second, once FoxP3$^-$ T cells are infected with HTLV-1, HBZ should be expressed in the host cells. Since HBZ is recently

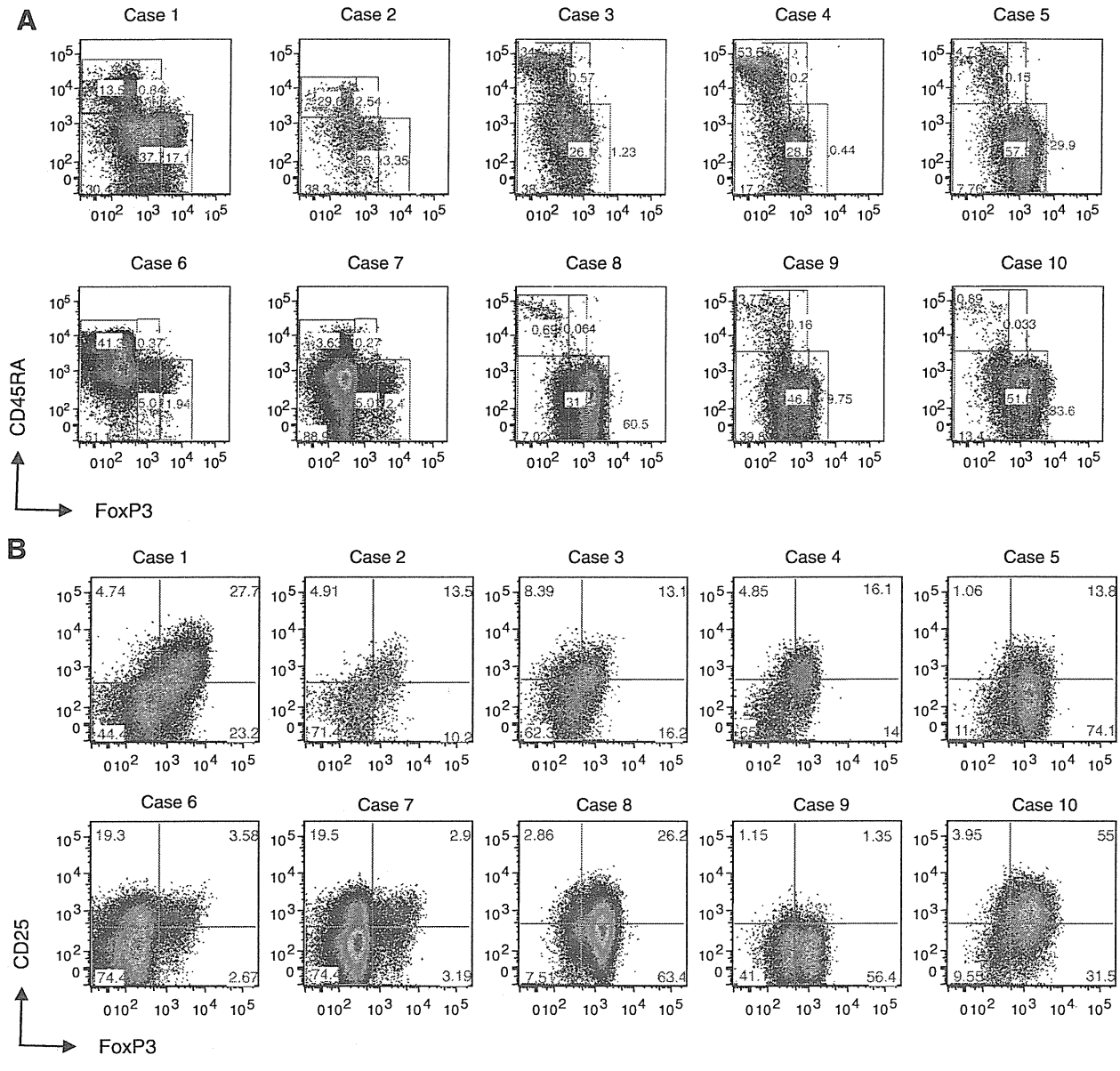

Figure 6 Characterization of CD4$^+$ T-cell subsets in ATL cells. PBMCs from ATL patients (n = 10) were stained with anti-CD4, anti-CD45RA, anti-CD25, and anti-FoxP3 antibodies and analyzed by flow cytometry. **(A)** The expression pattern of CD45RA and FoxP3 of CD4$^+$ T cells in ATL patients. **(B)** The expression pattern of CD25 and FoxP3 of CD4$^+$ T cells in ATL patients.

reported to induce FoxP3 expression via enhancing TGF-β signaling pathway [17,40], HTLV-1 infection is likely to convert FoxP3$^-$ cells into FoxP3$^+$ cells. In addition, HTLV-1 has a cell-extrinsic effect on FoxP3$^+$ cell generation. HTLV-1 infected cells secrete CCL22 via expression of Tax, which indirectly contributes to the generation and maintenance of HTLV-1 uninfected FoxP3$^+$ cells [41,42]. This would contribute to an increased number of HTLV-1-uninfected FoxP3$^+$ cells.

Since FoxP3$^+$ T_{reg} cells play a crucial role in suppressing immune response, the increase of FoxP3$^+$ cells observed in HTLV-1 infection may contribute to immunodeficiency, which is frequently observed in HTLV-1 infection [43]. On the other hand, the high frequency of FoxP3$^+$ T cells observed in HAM/TSP patients is paradoxical, because the pathogenesis of HAM/TSP is believed to be inflammatory. Therefore, we analyzed the phenotype of the increased FoxP3$^+$ cells and observed that CTLA-4 and GITR expression of FoxP3$^+$ T cells in HAM/TSP patient was significantly reduced compared to uninfected individuals (Figure 5C). A similar observation was reported previously that the expression level of

FoxP3, GITR, or CTLA-4 mRNA in $CD4^+CD25^+$ T cells of HAM/TSP patients is lower than that of HD [44]. That report used $CD4^+CD25^+$ as a marker of T_{reg} cells, but $CD4^+CD25^+$ T cells contain not only $FoxP3^+$ T_{reg} cells but also $FoxP3^-$ activated T cells. Particularly the proportion of $CD4^+CD25^+FoxP3^-$activated T cells is up-regulated in HAM/TSP patients, which is likely to reduce the proportion of $FoxP3^+$ T_{reg} cells in $CD4^+CD25^+$ T cells of HAM/TSP patients. Thus, the expression level of GITR or CTLA-4 in $FoxP3^+$ T cells of HAM/TSP patients has not been elucidated yet. To avoid this concern, we utilized the multicolor flow cytometry, which enabled us to show that CTLA-4 and GITR were clearly down regulated in $FoxP3^+$ T cells of HAM/TSP patients.

Then what is the underlying mechanism of this phenomenon? We reported recently that HBZ-Tg mice showed a pro-inflammatory phenotype in spite of the increase of $Foxp3^+$ T cells [17], which is similar to HAM/TSP patients (Figure 1D). T_{reg} associated molecules were also down regulated in $Foxp3^+$ T cells of HBZ-Tg mice. Thus, HBZ-mediated FoxP3 dysfunction may play a role in the abnormality regarding $FoxP3^+$ cells in HAM/TSP patients. It has been reported that Tax also contributes to the dysregulation of $FoxP3^+$ T_{reg} cells. Tax suppresses FoxP3 expression at transcriptional level [45], which alternatively or additionally could contribute to the abnormal phenotype of $FoxP3^+$ cells. These findings collectively indicate that the increased $FoxP3^+$ T_{reg} cells were functionally impaired in HAM/TSP patients. Furthermore, $FoxP3^+$ $CD4^+$ T cells in HAM/TSP patient contain an increased $FoxP3^+$ non-Treg population (Figure 5F), which would contribute to the inflammatory phenotype of HAM/TSP via generation of pro-inflammatory cytokine-producing $CD4^+$ T cells such as T_{HAM} cells [46] or exFoxp3 cells [47].

In the current study, we did not observed FoxP3 repression during Tax expression by *ex vivo* cultivation. This result seems to be inconsistent with a previous report that Tax represses FoxP3 expression [45]. There are two possible explanation of this inconsistency. First, there is the difference of the ways to express Tax. In the previous study, the authors used transfection of plasmid that induces Tax expression by the CMV promoter. We used endogenous HTLV-1 provirus to express Tax. Therefore, the expression level of Tax in our current study should be much lower than that of the previous study. In addition, Tax expression was induced in a proportion of $FoxP3^+$ cell in our current study. Second, there are differences in incubation time for Tax expression. In the previous study, the authors evaluated FoxP3 expression after 48 hours of transfection, whereas we evaluated FoxP3 expression within 24 hours after Tax expression.

High expression levels of CD25 are also well documented in HTLV-1 infection [33]. Consistent with previous findings, CD25 expression is upregulated in $FoxP3^+$ cells of HAM/TSP patient (Figure 5C). One determinant of the susceptibility to HAM/TSP is host genetic polymorphism such as MHC class 1, which influences the efficiency of CTL against HTLV-1 [48,49]. HTLV-1-infected individuals who have HLA class I susceptible for HAM/TSP may allow high expression of Tax and/or HBZ, which could cause up-regulation of CD25 molecules in the $FoxP3^+$ cell population (Figure 5C).

It is controversial whether ATL is a leukemia of $FoxP3^+$ T_{reg} cells or not. However, there is no *a priori* reason to assume that ATL cells must be exclusively derived from $FoxP3^+$ T_{reg} cells or non-T_{reg} cells. Indeed, there are previous reports to support both possibilities. Some studies have reported that ATL cells have regulatory functions [50,51], whereas other studies reported no regulatory function in ATL [52,53]. We showed here that HTLV-1 is frequently detectable in $CD4^+FoxP3^+$ T cells (Figure 3B) in AC. More than half of ATL cells express FoxP3 (Figure 6), even though FoxP3 expression in ATL cells is variable as shown in the present and previous studies [30,31]. These findings prompt us to propose an idea that more than a half of ATL cells are possibly derived from $FoxP3^+$ T_{reg} cells. We reported previously that HBZ expression is constitutively active but Tax expression is frequently silenced in ATL cells, which possibly contributes to high frequency of $FoxP3^+$ ATL.

Conclusion

This study demonstrated that HTLV-1 infection induced the abnormality of frequency and phenotype of $FoxP3^+$ T cells, suggesting that HTLV-1 has evolved a sophisticated strategy to achieve persistent infection by directly affecting the central regulator of the host immune system. HTLV-1-mediated dysregulation of $FoxP3^+$ T cells is likely to be a critical cellular mechanism for the understanding HTLV-1 pathogenicity.

Methods

Clinical samples and ethics statement

PBMCs were obtained from asymptomatic HTLV-1 infected carriers (n = 23), HAM/TSP patients (n = 10), ATL patients (n = 10), and age-matched healthy controls (n = 10). Characteristics of each group are presented in Table 1. ATL patients consist of 2 acute, 4 smoldering and 4 chronic types of ATL cases. Genomic DNA extracted from PBMCs was used to determine proviral load (PVL) as described previously [29]. Briefly, PVL was quantified by real time PCR and calculated by using genomic DNA of TL-Om1, an ATL cell line with one copy of complete HTLV-1 provirus, as a standard of 100%. We defined AC with less than 2% of proviral load as AC^{low} and AC with more than 2% of proviral load as AC^{high}. This study was conducted according to the